Fuel 382 (2025) 133657

Contents lists available at ScienceDirect

Fuel

journal homepage: www.elsevier.com/locate/fuel

Full Length Article

Catalytic and kinetic investigation into 4-dimethylamino pyridine/1,3-diphenyl thiourea catalyzed synthesis of chloromethyl ethylene carbonate under pure CO_2 and simulated flue gas conditions

Udeme O. Eton [a,b], Will Meredith [a], Colin E. Snape [a,*]

[a] Low Carbon Energy and Resources Technologies Group, Faculty of Engineering, University of Nottingham, Nottingham, NG7 2TU, United Kingdom
[b] Department of Chemical/Petrochemical Engineering, Akwa Ibom State University, Mkpat Enin LGA, Akwa Ibom State, Nigeria

ARTICLE INFO

Keywords:
CO_2 utilization
Cyclic carbonate
Hydrogen bond donor
Kinetics
Catalytic
Flue gas

ABSTRACT

Synthesis of chloromethyl ethylene carbonate (CMEC) via CO_2 cycloaddition to epichlorohydrin (ECH) has been investigated using a simple metal-free and halide-free catalyst comprising 4-dimethylamino pyridine (DMAP) and N–H type hydrogen bond donors (HBDs). Combining DMAP and 1,3-diphenyl thiourea (DPTU) had the strongest synergistic effect, which resulted in the highest improvement in CMEC yield. DMAP/DPTU was active in the presence of a simulated flue gas (15 % $C0_2$ in N_2) at low temperatures (30 – 60 °C), reaching a high CMEC yield (93 %) and selectivity (98 %) at 40 °C in 24 h. The presence of O_2 in simulated flue gas had no effect on catalytic activity; however, excessive H_2O in the reactor had a negative effect, resulting in low yield and selectivity. The reaction obeyed pseudo-first-order kinetics in terms of ECH, DMAP, and DPTU concentrations. The addition of DPTU increased the observed rate constant (k_{obs}) by a factor of 1.52 while decreasing the activation energy (E_a) of the reaction by 7.37 kJ/mol, indicating that the synergistic action of DPTU (HBD) and DMAP (nucleophile) influenced catalytic performance. The positive enthalpy ($\Delta H^{\ddagger}$) and Gibbs free energy ($\Delta G^{\ddagger}$) values indicate an endergonic and kinetically controlled reaction.

1. Introduction

Carbon dioxide (CO_2) is a viable and attractive C_1 building block for organic synthesis due to its renewability, abundance, nontoxicity, and low cost. As a result, CO_2 valorization into valuable chemicals is currently receiving great attention as an important technology for a sustainable chemical industry [1–5]. It can help decrease the chemical industry's reliance on petrochemicals as a feedstock [6]. It also offers a way to reuse a portion of the enormous amount of waste CO_2 present in industrial flue gases, which can help in reducing CO_2 emissions and related climate change [7,8]. To reuse waste CO_2 for chemical synthesis, it is desirable and beneficial to directly utilize flue gas as an impure source of CO_2 without prior CO_2 separation and compression. This strategy will eliminate the need for energy-intensive and costly CO_2 capture and regeneration [9,10].

A potentially effective process pathway for CO_2 chemical reuse is the cycloaddition of CO_2 to epoxides to obtain cyclic carbonates. Given the thermodynamic stability of CO_2 which is associated with a high energy barrier for its activation [11], the highly exothermic nature of the reaction, high steric energy of the epoxide (co-reactant) and the low energy level of the cyclic carbonate product are thermodynamically advantageous factors. The cyclic carbonate product is a high-value chemical with wide industrial applicability [12–15]. However, cyclic carbonates are currently manufactured under high CO_2 pressure (30 – 100 atm) and high temperature (150 – 210 °C), making use of pure CO_2 gas [15]. The harsh reaction conditions require significant energy input for operation, raising the question of energy efficiency and the potential for net CO_2 emission. In contrast, a process that aims to directly utilize waste CO_2 in industrial flue gas for cyclic carbonate synthesis should require little or no energy input for heating or compression; otherwise, the process may become a net emitter of CO_2. Hence, the reaction should operate efficiently at atmospheric pressure and low temperature (< 100 °C). In addition, it is crucial for the process to maintain a reasonable reaction rate and chemical stability under typical flue gas conditions, which include low CO_2 partial pressure ($\leq$ 0.15 atm for coal-fired power plants) and the presence of reactive gases such as O_2, H_2O, and SO_2 etc [16,17].

Significant research efforts have been put into developing catalyst

* Corresponding author.
E-mail address: colin.snape@nottingham.ac.uk (C.E. Snape).

https://doi.org/10.1016/j.fuel.2024.133657
Received 27 February 2024; Received in revised form 21 October 2024; Accepted 5 November 2024
Available online 18 November 2024

systems that work under pure CO_2 conditions at atmospheric pressure and temperatures below 100 °C. Metal and/or halide-based catalysts are the most widely reported catalysts for this condition. One of the most active catalysts is the bifunctional organometallic complex/quaternary ammonium or phosphonium halide salt [18–27]. Another efficient class of catalysts for this condition is the hydroxyl-containing hydrogen bond donor (HBD)/quaternary ammonium or phosphonium halide salt bifunctional catalysts, such as dinaphthyl silanediol/tetrabutylammonium iodide (TBAI), 2-pyridine methanol/TBAI etc. [28–33]. Moreover, amines or amidines were protonated by halo acids (e.g. HI) to form bifunctional catalysts, such as triethylamine hydroiodide (Et_3N-HI), DBU hydroiodide (DBU.HI) etc., which was also capable of catalyzing cyclic carbonate synthesis from CO_2 and epoxides at atmospheric pressure and < 100 °C under pure CO_2 condition [34–36]. Metal halides and organic halides were also combined with organic bases (for instance, CaI_2/MDEA) to form active bifunctional catalysts for the reaction [37,38]. Furthermore, in terms of catalytic developments towards directly utilizing flue gas for cyclic carbonate synthesis, a few metal and halide-based bifunctional catalysts (mostly organometallic complex /quaternary ammonium halide catalysts) were applied to reactions involving a diluted CO_2 gas or actual flue gas; however, some of them required long reaction times of 48——96 h to attain high cyclic carbonate yield [26,37,39–43]. Despite some positive outcomes, the use of catalysts based on metals and halides has drawbacks for industrial use. These include contamination of the final product due to toxic metallic residues, difficult/costly disposal of hazardous metallic wastes, rigorous and expensive catalyst preparation, and corrosion of reactor components by halide salts.

Metal-free and halide-free catalysts were shown to produce high yields of cyclic carbonates only at high temperatures and CO_2 pressures. A Schiff base combined with 4-dimethylaminopyridine (DMAP) catalyzed the reaction of pure CO_2 and epichlorohydrin (ECH), affording 99 % yield of chloromethyl ethylene carbonate (CMEC) in 24 h at 120 °C and 35.2 atm CO_2 pressure in the presence of an organic solvent [44]. A binary catalyst comprising an organic base, 1,8-diazabicyclo[5.4.0] undec-7-ene and L-histidine catalyzed the reaction of pure CO_2 and ECH, achieving 88 % conversion of ECH in 2 h at 120 °C and 19.7 atm CO_2 pressure [45]. Poly (ionic liquid)s (PILs) are a promising class of metal-free catalysts for CO_2 capture and fixation applications. They incorporate the functional properties of ionic liquids into a polymeric framework, resulting in a tunable porous polymer which has attracted much attention in CO_2 cycloaddition to epoxides. Interest in PILs stems from their unique ability to combine abundant pores and basic sites for CO_2 enrichment/activation and nucleophilic sites for epoxide ring-opening [46,47]. Very recently, [48] reported a porous sulfonyl binuclear carbonate PIL which catalyzed CMEC synthesis in 98 % yield after 2 h from the reaction of ECH and a simulated flue gas containing 15 % CO_2 at 10 atm and 120 °C. Also, [49] demonstrated that a guanidine-functionalized binuclear PIL was effective in mediating 96 % yield of CMEC in 4 h from ECH and a simulated flue gas containing 15 % CO_2 at 20 atm and 100 °C. Metal-free and halide-free catalysts were scarcely reported under mild reaction conditions, apart from the recently reported phosphorous ylide CO_2 adduct [50], and PILs [47,51] which catalyzed the reaction in the presence of pure CO_2 at atmospheric pressure. It is, therefore, of interest to develop metal-free and halide-free catalytic methodologies that can achieve high reaction rates that ensure a high reactor throughput under atmospheric pressure and low temperatures, not only under pure CO_2 conditions but also under typical flue gas conditions.

Herein, we report a simple metal-free and halide-free binary catalyst, which demonstrates for the first time, the existence of a positive synergy between a nucleophilic base and N–H type hydrogen bond donor (HBD) to catalyze cyclic carbonate synthesis from CO_2 and epoxide. The cycloaddition of ECH with CO_2 to produce the cyclic carbonate, CMEC (Scheme 1) was selected as the model reaction to explore the catalytic activity of the binary catalyst. More importantly, the optimum catalyst,

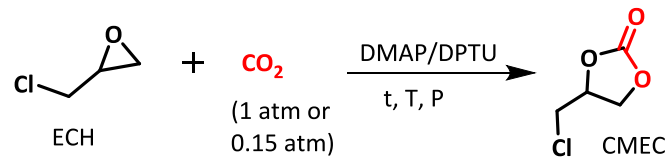

Scheme 1. Synthesis of CMEC by the CO_2 Cycloaddition to ECH.

comprising DMAP and 1,3-diphenyl thiourea (DPTU), could facilely mediate the formation of CMEC in high yields from ECH and CO_2 under mild conditions (1 or 0.15 atm CO_2 partial pressure and ≤ 60 °C). Further testing of the DMAP/DPTU binary catalyst was carried out under a simulated flue gas atmosphere to assess the influence of CO_2 partial pressure and major flue gas impurities (O_2 and H_2O) on reaction efficiency; and for the first time, a metal-free and halide-free catalyst exhibits high catalytic activity under 0.15 atm CO_2 partial pressure to afford a high yield of cyclic carbonate at a relatively low temperature of 40 °C. Finally, the influence of the catalytic components on the reaction rate was measured and the catalytic role of the catalyst components was elucidated, by kinetic studies.

2. Experimental

2.1. Reagents

The following chemicals were used in this research. Epichlorohydrin, ECH (99 %), 4-dimethylamino pyridine, DMAP (99 %), and propylene carbonate, PC (99.5 %) were purchased from ACROS Organics, Belgium. 1-methyl naphthalene (99 %), chloromethyl ethylene carbonate, CMEC (> 99 %), and deuterated chloroform ($CDCl_3$) were purchased from Sigma-Aldrich Company Ltd., UK. Dichloromethane, DCM (99.9 %), 1,3-diphenyl urea, DPU (98 %), thiourea (99 %), urea (99.3 %), and 1,3-diphenyl thiourea, DPTU (99 %) were purchased from Fisher Scientific Ltd., UK. Pure CO_2 gas (99.99 %), 15 % CO_2/85 % N_2 mixture, and 15 % CO_2/5 % O_2/80 % N_2 mixture were supplied by BOC Limited, UK. The purity of all the chemicals was verified by gas chromatography (GC) analysis. All chemicals were used as received without further purification.

2.2. Instrumentation

An Agilent 7890B GC system was used for GC analysis. The GC system was equipped with a flame ionization detector (FID) and an RTX-1701 capillary column coated with 14 % cyanopropylphenyl/86 % dimethylpolysiloxane (60 m x 0.32 m x 1 μm). The peaks of known compounds were assigned on the GC chromatogram by comparing the retention times with that of authentic commercial samples analyzed under identical GC conditions, while unknown compounds and their retention times were determined by GC–MS analysis. GC–MS analysis was carried out on an Agilent 7890B GC system/5977A MSD analyzer under 70 eV electron impact ionization and full scan mode. ^1H and ^{13}C NMR spectra were obtained from a 400 MHz Bruker NMR spectrometer with deuterated chloroform ($CDCl_3$) as the solvent. Chemical shifts (δ) were reported in ppm relative to the $CHCl_3$ residual peak in $CDCl_3$ (at 7.26 ppm) for ^1H NMR spectra or relative to the middle peak of the triplet $CDCl_3$ peak (at 77.16 ppm) for ^{13}C NMR spectra. Signal multiplicities were abbreviated as s (singlet), d (doublet), t (triplet), q (quartet), and m (multiplet).

2.3. General Procedure for synthesis of chloromethyl ethylene carbonate (CMEC)

All the reactions were carried out in a 100-mL three-neck glass flask (reactor). In a typical operation, the reactor was charged with DMAP (0.60 g, 5.0 mmol), DPTU (0.15 g, 0.66 mmol), and ECH (7.5 g, 81.1

mmol) successively at room temperature. The mixture was continuously stirred by a magnetic stirrer; and when the DMAP and DPTU dissolved completely, the reactor was heated by an oil bath/hotplate equipped with a thermostat for temperature control. When the desired reaction temperature of 60 °C was attained, pure CO_2 gas at a pressure and feed rate of 1 atm and 4 ml/min respectively, was bubbled through the mixture. During the reaction, pure CO_2 gas was continuously charged into the reactor through a pressure regulator and mass flow controller (*Alicat/MC-100SCCM-D*) to maintain pressure and feed rate at the desired setpoint. For reactions with simulated flue gas, the pure CO_2 gas supply was replaced with a 15 % CO_2/85 % N_2 or 15 % CO_2/5 % O_2/80 % N_2 gas mixture flowing at a pressure and flowrate of 1 atm and 26.7 ml/min, respectively. The reaction progress was monitored by withdrawing an aliquot of the reaction mixture at 1-hour intervals and dissolving it in DCM for GC analysis. The reaction components could be separated using differences in solubility and boiling point. DMAP, which is water-soluble, was separated from water-insoluble CMEC and DPTU by constantly stirring the reaction mixture in water at 60 °C and then decanting the aqueous and organic phases. DMAP was recovered from the aqueous phase using vacuum evaporation. The reaction product, CMEC (normal boiling point = 290.1 °C), could be easily isolated from the organic phase by vacuum evaporation in a rotary evaporator (80 °C, 6 mbar), leaving DPTU (normal boiling point = 348.7 °C) solid in the flask. The structure/purity of the reaction product was identified by GC–MS and $^1H/^{13}C$ NMR techniques (***See Supplementary Material, Figures S1-S2***). $^1H/^{13}C$ NMR characterizations of the synthesized CMEC completely matched those reported in the literature [36,52,53]. The $^1H/^{13}C$ spectral data of the synthesized CMEC were as follows: ^1H NMR (400 MHz, $CDCl_3$) δ_H (ppm): 5.01 − 4.96 (m, 1H, ring OCH), 4.58 (t, J = 8.9 Hz, 1H, ring OCH_2), 4.38 (dd, J = 8.9, 5.7 Hz, 1H, ring OCH_2), 3.81 − 3.70 (m, 2H, CH_2Cl); ^{13}C NMR (101 MHz, $CDCl_3$) δ_C (ppm): 154.39 (C = O), 74.43 (OCH), 67.03 (OCH_2), 43.97 (CH_2Cl).

2.4. Determination of catalytic performance

Catalytic activity was defined in terms of conversion, yield, and selectivity according to **Equations (1) – (3)** [54]. Conversion, yield, and selectivity were determined by GC analysis of the reaction mixtures [55,56] using the internal standard quantitation method, with 1-methyl naphthalene as the standard.

$$Conversion = \frac{|\Delta n_{ECH}|}{(n_{ECH})_i}.100\% \quad (1)$$

$$Yield = \frac{n_{CMEC}}{Theoretical\ n_{CMEC}}.100\% \quad (2)$$

$$Selectivity = \frac{n_{CMEC}}{|\Delta n_{ECH}|}.100\% \quad (3)$$

The fraction of CO_2 passing through the reaction mixture that was fixed into the CMEC product, denoted as CO_2 utilization, was defined according to **Equation (4)**:

$$CO_2 Utilization = \frac{n_{CMEC}}{n_{CO2fed}}.100\% \quad (4)$$

Where, $\Delta n_{ECH} = (n_{ECH})_o - n_{ECH}$, $(n_{ECH})_o$ is the initial number of moles of ECH (mol), n_{ECH} is the number of moles of unreacted ECH (mol), and n_{CMEC} is the actual number of moles of CMEC in the reaction mixture (mol). n_{ECH} and n_{CMEC} were quantified by measuring the ECH and CMEC GC peak areas, respectively from the chromatogram of the reaction mixtures and then applying the GC internal standard quantitation method, which was described elsewhere [57,58]. A GC internal standard calibration curve (***See Supplementary Material, Figures S7 – S9***) was constructed for ECH and CMEC from standard solutions of different concentrations, which allowed ECH and CMEC concentrations in the reaction mixture to be determined as a function of peak area ratio. The GC analytical method was validated as per the ICH guidelines [59].

2.5. General Procedure for kinetic studies

ECH (81.1 mmol or 45.4 mmol), DMAP (8.0, 5.0, 2.5, or 1.5 mmol), and DPTU (0.99, 0.66, 0.41, or 0.25 mmol) were dissolved in propylene carbonate (PC) and the volume of the solution was made up to 10 ml with PC. The cycloaddition reaction was carried out at T = 40 – 80 °C under a continuous supply of pure CO_2 gas or simulated flue gas (15 % CO_2/85 % N_2). For each experiment, samples were taken from the reaction mixture every 30 min and analyzed by GC to obtain concentration–time data to construct the reaction profile.

3. Results and discussions

3.1. HBD Screening

The catalytic activity of DMAP in the presence of N–H type HBDs, namely urea, thiourea, 1,3-diphenyl urea (DPU), or 1,3-diphenyl thiourea (DPTU), was investigated and the corresponding results are presented in Table 1.

No products were detected when the cycloaddition of CO_2 to ECH was performed in the absence of both DMAP and DPTU at 60 °C and 1 atm CO_2 pressure. Similarly, no products were detected when only the N–H type HBDs were used as catalysts for the reaction at 60 °C and 1 atm CO_2 pressure.

However, when DMAP alone, at a ratio of 0.1 w/w relative to ECH, was used as the catalyst, CMEC yield and selectivity of 62 % and 99 %, respectively were observed after 5 h at 60 °C and 1 atm CO_2 pressure (Table 1, **Entry 1**). By substituting a portion of DMAP with the N–H type HBDs, a bifunctional catalyst was formulated such that the influence of the HBDs on the reaction could be investigated while retaining the same catalyst concentration as when DMAP was used alone. Interestingly, the resulting binary catalysts were more active than DMAP alone, leading to an obvious enhancement of the reaction rate between CO_2 and ECH. Consequently, the DMAP/N–H HBD binary catalysts exhibited higher CMEC yields (80——89 %) than was obtained for DMAP only under identical reaction conditions (Table 1, **Entries 2 – 5**). The catalytic activity of the DMAP/ N–H HBD binary catalysts increased according to the order: DMAP/urea < DMAP/DPU ≈ DMAP/thiourea < DMAP/DPTU. DMAP/DPTU emerged as the optimum catalytic combination affording CMEC yield and selectivity of 89 % and 99 %, respectively after 5 h of reaction at 60 °C and 1 atm CO_2 pressure. Extending the reaction duration to 8 h further demonstrated the efficacy of DPTU to accelerate CMEC synthesis as the DMAP/DPTU catalyzed reaction quickly approached completion, affording a CMEC yield of 94 %, while the reaction catalyzed by DMAP only afforded a CMEC yield of 69 %; however, CMEC selectivity remained at 99 % in both cases (Table 1,

Table 1
Screening of N–H Type HBDs as Promoters [a.]

Entry	Base	HBD	Yield (%) [b]	Selectivity (%) [b]	Conversion (%)[b]
1 [c]	DMAP	–	62	99	63
2	DMAP	Urea	80	97	82
3	DMAP	Thiourea	85	92	92
4	DMAP	DPU	84	97	87
5	DMAP	DPTU	89	99	90
6 [d]	DMAP	–	69	99	70
7 [d]	DMAP	DPTU	94	99	95

[a] – reaction conditions: ECH = 7.5 g, Catalyst/ECH weight ratio = 0.1, DMAP: HBD = 3:1, T = 60 °C, t = 5 h, p_{CO_2} = 1 atm, pure CO_2, $\dot{f}_{CO_2}$ = 7.5 ml/min;
[b] – determined by GC technique;
[c] – reaction catalyzed by DMAP only, but with DMAP/ECH weight ratio = 0.1;
[d] – reaction time, t = 8 h.

Entries 6 – 7). DMAP is known to be a nucleophilic base [60,61] due to the presence of lone pairs of electrons on the N-atom of its phenyl ring which attacked and opened the epoxide ring to encourage CO_2 insertion. Thus, the reaction could not occur in its absence. The improvement in CMEC yield with the DMAP/ N–H type HBD binary catalysts therefore suggests that the synergy between a nucleophilic specie and the hydrogen bonding amino (N–H) moiety exerted a positive effect on the ring opening of ECH to accelerate the formation of CMEC. Fig. 1 provides a comparison of the time-dependent profiles of CMEC yield and selectivity obtained for the reactions catalysed by DMAP/N–H type HBDs which further illustrates the relative promoting influence of these HBDs in accelerating the reaction.

3.2. Synthesis of CMEC under simulated flue gas atmosphere

Pure CO_2 gas was replaced with a simulated flue gas stream to investigate the reaction efficiency when DMAP/DPTU is applied as a catalyst under a post-combustion flue gas environment. A simulated flue gas stream containing 15 % CO_2 (v/v) in N_2 at 1 atm was used while reactions were conducted at low temperatures (30 – 60 °C). The results obtained are shown in Fig. 2. The DMAP/DPTU binary catalyst retained its catalytic activity under 0.15 atm CO_2 partial pressure at low temperatures of 30 – 60 °C and CMEC formation under the simulated flue gas atmosphere proceeded seamlessly resulting in complete ECH conversion at T ≥ 50 °C after 24 h, as confirmed by GC data (***See Supplementary Material, Figure S3***). When the reaction was allowed to proceed for 24 h, CMEC yield of 67 %, 93 %, 96 %, and 97 % was obtained at temperatures of 30 °C, 40 °C, 50 °C, and 60 °C, respectively. These results show that CMEC yield generally increased with increasing temperature, however, it is of practical interest that a high yield of CMEC was obtained at a low temperature of 40 °C by the catalytic action of DMAP/DPTU under 0.15 atm CO_2 partial pressure. Generally, the reactions under 0.15 atm CO_2 partial pressure proceeded with excellent selectivity towards CMEC formation (≥ 97 %) and CMEC selectivity remained fairly independent of reaction temperature.

Previously, only catalysts based on metal–organic complexes and/or halide salts were shown to be effective in the cycloaddition of diluted or waste CO_2 to epoxides to synthesize cyclic carbonates. For instance, Hui *et al.*[41] reported a mesoporous porous ionic copolymer, poly (divinylbenzene-1-allyl-tetramethylguanidinium) bromide which achieved an ECH conversion of 92 % at 100 °C and 15 % CO_2 after 48 h of reaction. Similarly, when either the homogeneous cobalt tetraphenylporphyrin complex or heterogeneous cobalt-doped porous organic tetraphenylporphyrin polymer were used in combination with tetrabutylammonium bromide, 37.4 % or 45.4 % conversion of ECH, respectively were obtained after 48 h at 29 °C and 15 % CO_2 [39]. A homogeneous bimetallic Al(salen) complex/tetrabutylammonium bromide binary catalyst was reported to catalyze the reaction of ECH and flue gas containing 5 % v/v waste CO_2, achieving 100 % ECH conversion in 83.3 hr at 26 °C [42]. A multifunctional CaI_2/n-methyldiethanolamine catalyzed the synthesis of styrene carbonate from styrene oxide and a 15 % diluted CO_2, achieving 88 % conversion of styrene oxide in 24 h at 50 °C [37]. A poly(4-vinylphenol)/ tetrabutylammonium iodide system achieved 25 % conversion of hexene oxide in 22 h at 40 °C, when a CO_2/N_2 mixture containing ≈ 10 % CO_2 v/v was used [62]. Li *et al.* [63] employed a binary catalyst comprising of 2-phenylimidazolinium based porous ionic polymer and $ZnBr_2$ to catalyze the reaction of ECH and 15 % diluted CO_2 at 55 °C and reported a 96 % conversion of ECH after 120 h. The use of metal- and halide-based catalysts poses a serious challenge for large-scale practical implementation owing to the corrosiveness of halide salts and the risk of product contamination by metallic residues. Besides, most of the catalysts still required 48 h or longer to achieve high conversions at temperatures < 100 °C, despite the presence of costly/exotic metal–organic complexes. In contrast, the metal-free and halide-free DMAP/DPTU bifunctional catalyst reported in the present work achieved a 95 % conversion of ECH in 24 h at 40 °C and 15 % diluted CO_2, presenting a bright prospect for large-scale practical application.

Fig. 3 illustrates the influence of CO_2 partial pressure on the catalytic performance of DMAP/DPTU binary catalyst by comparing the time-resolved reaction profile at 60 °C under pure CO_2 (CO_2 partial pressure, $pCO_2 = 1$ atm) and simulated flue gas (CO_2 partial pressure, $pCO_2 = 0.15$ atm) conditions. The result shows a decrease in CMEC yield as CO_2 partial pressure decreased from 1 atm to 0.15 atm, while the selectivity towards CMEC formation remained unaffected by CO_2 partial pressure. This suggests that while the reaction rate between CO_2 and ECH was altered by a change in CO_2 partial pressure, the reaction pathway remained unchanged.

3.3. Effect of flue gas impurities on CMEC synthesis

It was of interest to investigate what effect, if any, the reactive impurities in flue gas might have on the activity of the DMAP/DPTU binary catalyst. Modern power plants encompass pollution control technologies [64] that can remove SO_x, NO_x, and particulate matter completely or to a very low concentration (10 – 70 ppm for SO_2 and 50 – 100 ppm for NO_x in the case of coal-fired power plants) [65], leaving water vapour and O_2 as the major impurities. The effect of O_2 was investigated by bubbling a simulated flue gas stream comprising 15 % CO_2/5 % O_2/80 % N_2 (v/v) at 1 atm through a mixture of ECH and the catalyst in the reactor. The results obtained for reactions carried out in the presence of O_2 were compared to those carried out in the absence of O_2 as presented in Fig. 4.

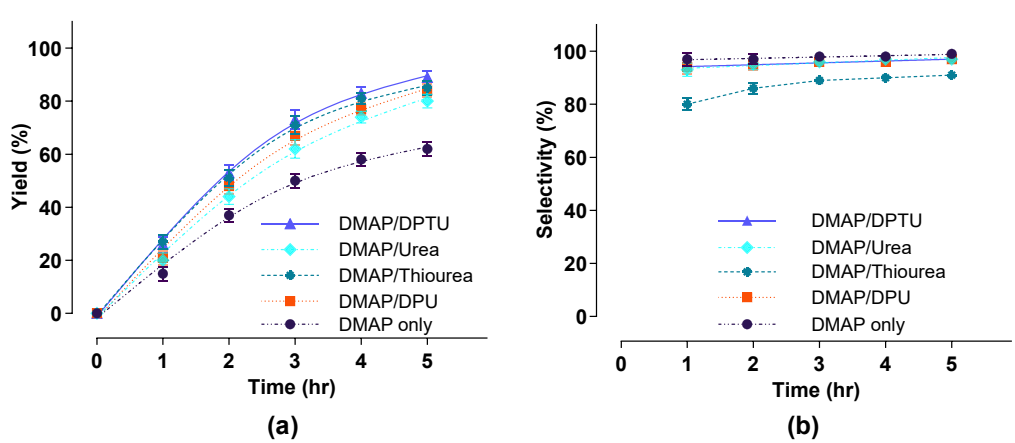

Fig. 1. Time-dependent profiles for reactions catalyzed by DMAP/N–H type HBD binary catalysts: (a) yield (b) selectivity. Reaction conditions: ECH = 7.5 g, Catalyst/ECH weight ratio = 0.1, DMAP: HBD = 3:1, T = 60 °C, t = 5 h, p_{CO_2} = 1 atm, Pure CO_2, $\dot{f}_{CO_2}$ = 7.5 ml/min. Error bar represents the standard deviation.

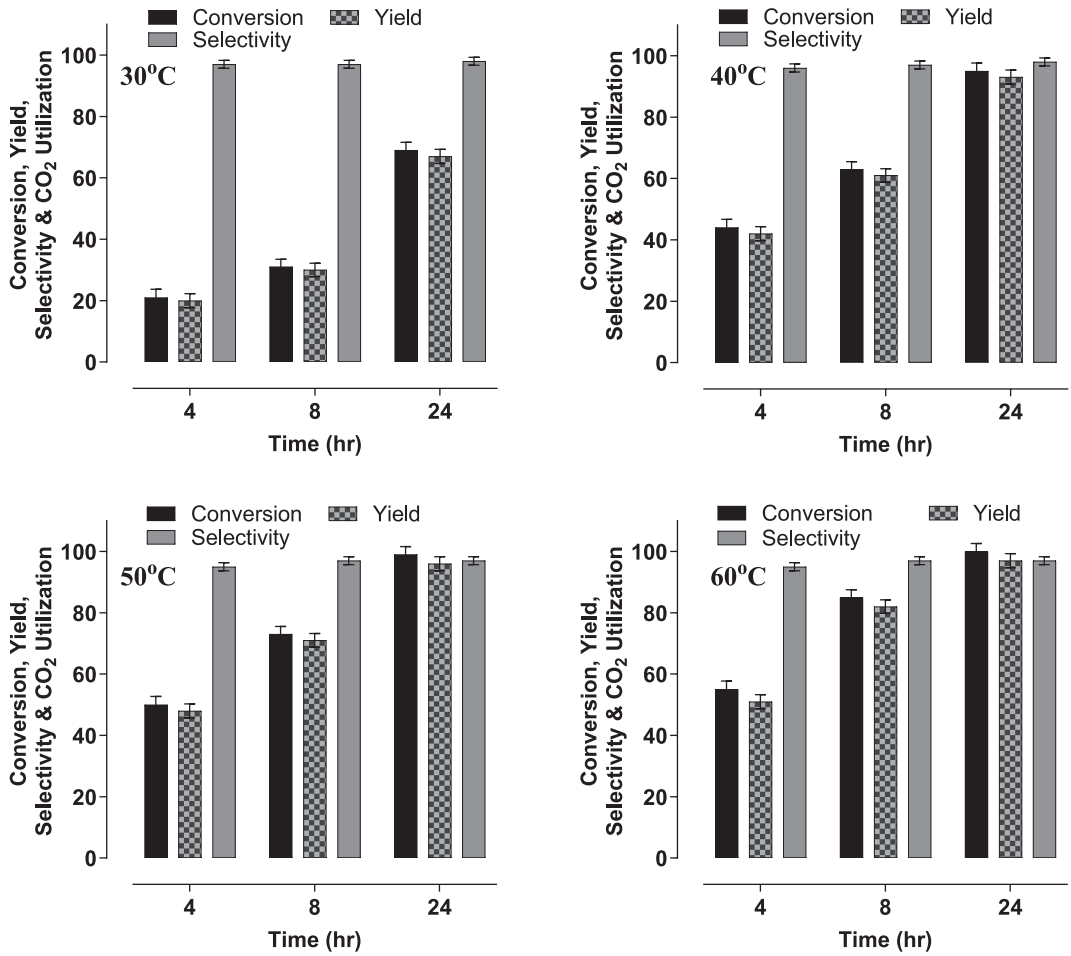

Fig. 2. DMAP/DPTU catalyzed synthesis of cyclic carbonate under simulated flue gas atmosphere at low temperatures. Other reaction conditions: ECH = 7.5 g, Catalyst/ECH weight ratio = 0.1, DMAP: DPTU = 4:1, 15 % CO_2/85 % N_2 (v/v), p_{CO_2}= 0.15 atm.$\dot{f}_{CO_2}$ = 4 ml/min, $\dot{f}_{total}$= 26.7 ml/min. Error bar represents the standard deviation.

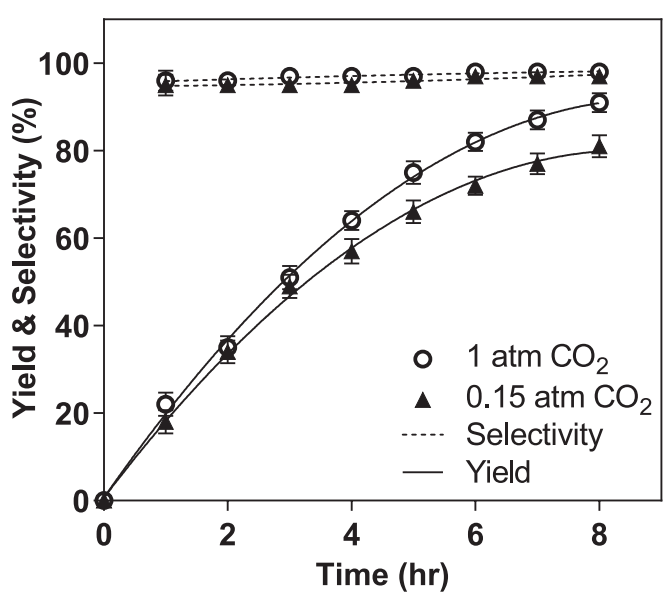

Fig. 3. Influence of CO_2 partial pressure on DMAP/DPTU catalyzed cycloaddition of CO_2 to ECH. Other reaction conditions: Epoxide = 7.5 g, Catalyst/ECH weight ratio = 0.1, DMAP: DPTU = 4:1, T = 60 °C, $\dot{f}_{CO_2}$= 4 ml/min. Error bar represents the standard deviation.

The concentration of O_2 in the simulated flue gas was chosen to meet the upper limit of the concentration range of O_2 in a typical flue gas from a coal-fired power plant, 3 – 5 % v/v [66].

It is evident from Fig. 4 that the catalytic activity of the DMAP/DPTU binary catalyst was not retarded under the oxidizing environment, therefore there was no significant difference in the yield of CMEC between reactions in the presence and absence of O_2 after 24 h. At 60 °C, a CMEC yield of 93 % was obtained in the presence of O_2 while the CMEC yield remained at 96 % in the absence of O_2 after 24 h. Also, at 30 °C, a CMEC yield of 80 % was obtained in the presence of O_2 while its value was 67 % in the absence of O_2 after 24 h. Also, despite that O_2 is a powerful oxidizing agent, its presence in the reaction system did not interfere with the reaction pathway. The reactions in the presence or absence of O_2 produced the CMEC with trace amounts of 3-chloropropane-1,2-diol (3-CPD) as the only reaction products. Therefore, CMEC selectivity was 98 % in the presence or absence of O_2. These results indicate that the DMAP/DPTU binary catalyst retained its activity and selectivity when exposed to an oxidizing environment.

Furthermore, it was observed that the presence of H_2O in the reactor at a concentration of 0.025 w/w relative to ECH led to a decrease in CMEC yield and selectivity compared to the reaction in the absence of H_2O. CMEC selectivity decreased from 99 % to 92 % due to a higher rate of formation of 3-CPD in the presence of H_2O. A further increase in H_2O concentration to 0.50 w/w relative to ECH resulted in a further decrease in CMEC yield and selectivity to 55 % and 75 %, respectively. Although the catalyst maintained some activity in the presence of H_2O, an excessive amount of H_2O in the reactor had a negative effect on the

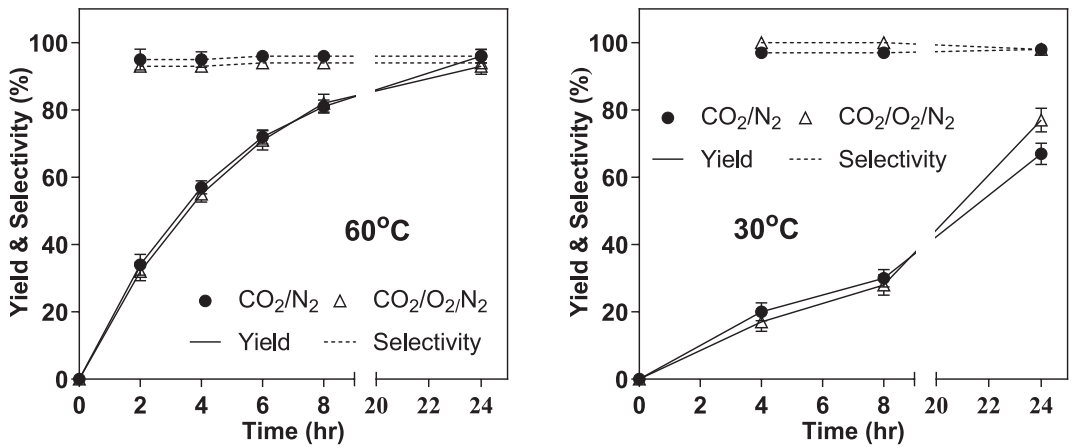

Fig. 4. Influence of O_2 in flue gas on CMEC synthesis by DMAP/DPTU binary catalyst. Other conditions: [ECH = 7.5 g, Catalyst/ECH weight ratio = 0.1, DMAP: DPTU = 4:1, pCO_2 = 0.15 atm, $\dot{f}_{CO_2}$= 4 ml/min, $\dot{f}_{total}$= 26.7 ml/min. Error bar represents the standard deviation.

catalytic activity due to dilution effect and formation of 3-CPD through the hydrolysis of ECH. Therefore, for real flue gas application, it would be necessary to cool the flue gas below its dew point to induce the condensation of water vapour before the flue gas is fed to the reactor. This will prevent excessive condensation of water vapour in the reactor which could decrease ECH conversion and CMEC selectivity.

3.4. Kinetics and Mechanistic studies

A Kinetics study was conducted to understand the influence of catalytic components and reaction conditions on the DMAP/DPTU catalyzed reaction and to evaluate the role of the catalytic components in the underlying reaction mechanism.

The general rate equation for CMEC formation by CO_2 cycloaddition to ECH can be written as shown in **Equation (5)**.

$$-\frac{d[ECH]}{dt} = k_{obs}[ECH]^a \tag{5}$$

$$k_{obs} = k[CO_2]^b[DMAP]^c[DPTU]^d \tag{6}$$

$$In[ECH] = -k_{obs}t + In[ECH]_o \tag{7}$$

$$Ink_{obs} = Ink + bIn[CO_2] + cIn[DMAP] + dIn[DPTU] \tag{8}$$

Where a, b, c, and d are the reaction order with respect to [ECH], [CO_2], [DMAP], and [DPTU], respectively. **Equations (5) and (6)** assume that DMAP concentration, [DMAP], DPTU concentration, [DPTU], and CO_2 concentration, [CO_2] are constant during each reaction. This is reasonable since DMAP and DPTU are catalytic reagents, and CO_2 is fed continuously to the reactor in excess [67,68]. The observed rate constant (k_{obs}) and reaction order in [ECH] could be determined by **Equation (5)**, through the integrated rate law method. If the reaction obeys a pseudo first-order kinetics with respect to [ECH], that is a = 1, then the rate law is described by **Equation (7)** and k_{obs} can be determined from the slope of a linear plot of In [ECH] versus t [69,70]. Furthermore, **Equation (6)** was linearized to obtain **Equation (8)**, which allowed the reaction order in [DMAP] and [DPTU] to be determined from the slope of double logarithmic plots [71].

3.4.1. Reaction order in ECH concentration

Firstly, reactions were conducted using DMAP/DPTU and 100 % CO_2 under the reaction conditions: 60 °C, 8.11 mol/L ECH, 0.5 mol/L DMAP and 0.066 mol/L DPTU. Secondly, to clarify the influence of DPTU on reaction kinetics, reactions were conducted using DMAP only and 100 % CO_2 under the reaction conditions: 0.5 mol/L DMAP, 60 °C, 8.11 mol/L ECH. Thirdly, to elucidate the influence of CO_2 partial pressure on reaction kinetics, reactions were conducted using DMAP/DPTU and 15 % CO_2 under the reaction conditions: 60 °C, 8.11 mol/L ECH, 0.5 mol/L DMAP and 0.066 mol/L DPTU. In all three cases, the reaction exhibited pseudo first-order kinetics in ECH concentration as the kinetic plots revealed a linear relationship between In [ECH] and t (Fig. 5). The value of k_{obs} at 60 °C was 0.0067 min^{-1} for DMAP/DPTU binary catalyst and 100 % CO_2, 0.0044 min^{-1} for DMAP only and 100 % CO_2, and 0.0056 min^{-1} for DMAP/DPTU binary catalyst and 15 % CO_2. k_{obs} increased by a factor of 1.52 (from 0.0044 min^{-1} to 0.0067 min^{-1}) due to the addition of DPTU to the catalyst mix, which accounts for the observed increase in CMEC yield. In contrast, k_{obs} decreased by a factor of 0.84 (from 0.0067 min^{-1} to 0.0056 min^{-1}) due to the decrease in CO_2 partial pressure from 1 atm to 0.15 atm, in agreement with the observed decrease in CMEC yield between CO_2 partial pressure of 1 atm and 0.15 atm. Therefore, by analyzing experimental data under various reaction conditions, the influence of DPTU and CO_2 partial pressure on the reaction rate was determined.

3.4.2. Reaction order in DMAP concentration

The reaction order with respect to DMAP concentration was investigated by using a fixed DPTU concentration of 0.066 mol/L while varying DMAP concentration between 0.15 – 0.80 mol/L. All the

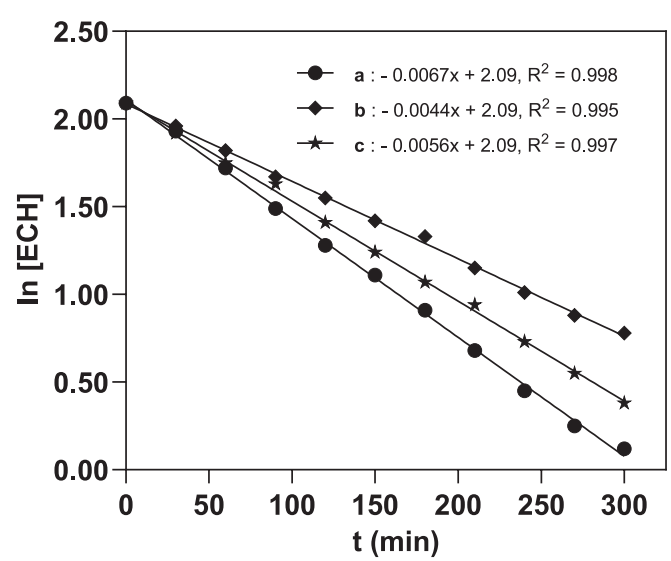

Fig. 5. Linear fit of In [ECH] versus t for reactions conducted at 60 °C in the presence of: (a) DMAP/DPTU binary catalyst and 100% CO_2, (b) DMAP alone as the catalyst and 100% CO_2, (c) DMAP/DPTU binary catalyst and 15% CO_2.

reactions were performed at 60 °C using 8.11 mol/L ECH and 100 % CO_2 (Fig. 6). As shown in Fig. 6**a**, all the experimental data exhibited a good fit to pseudo first-order kinetics with high R^2 values of ≥ 0.991. Thus, the values of k_{obs} were determined from the linear kinetic plots as 0.0020 min^{-1}, 0.0034 min^{-1}, 0.0067 min^{-1}, and 0.0106 min^{-1} for DMAP concentrations of 0.15 mol/L, 0.25 mol/L, 0.50 mol/L, and 0.80 mol/L, respectively. The rate of reaction between ECH and CO_2 increased with DMAP concentration within 0.15 – 0.80 mol/L. Furthermore, the reaction order with respect to DMAP concentration was determined from the plot of In k_{obs} against In [DMAP] as 1.003 (Fig. 6**b**), that is c = 1. This result suggests a reaction mechanism that involves one molecule of DMAP per molecule of ECH in the catalytic cycle.

3.4.3. Reaction order in DPTU concentration

Similarly, the reaction order with respect to DPTU concentration was investigated by using a fixed DMAP concentration of 0.5 mol/L, while varying DPTU concentration between 0.025 – 0.099 mol/L. All the reactions were performed at 60 °C using 8.11 mol/L ECH and 100 % CO_2 (Fig. 7). All the experimental data exhibited a good fit to pseudo first-order kinetics with high R^2 value of ≥ 0.982 (Fig. 7**a**). The values of k_{obs} were determined from the linear kinetic plots as 0.0022 min^{-1}, 0.0038 min^{-1}, 0.0067 min^{-1}, and 0.0082 min^{-1} for DPTU concentrations of 0.025 mol/L, 0.041 mol/L, 0.066 mol/L, and 0.099 mol/L, respectively. These results confirm the positive influence of N–H type HBD on the cycloaddition of CO_2 to ECH as the reaction rate increased with DPTU concentration. The reaction order with respect to DPTU concentration was determined from the plot of In k_{obs} against In [DPTU] (Fig. 7**b**) as 0.98, that is, d = 1. This result suggests the participation of one molecule of DPTU per molecule of ECH in the catalytic cycle.

3.4.4. Reaction Energetics

The temperature dependence of the reaction rate was modelled by Arrhenius and Eyring equations to determine the kinetics and thermodynamic activation parameters for the reaction [72,73].

$$k_{obs} = Ae(-E_a/RT) \tag{9}$$

$$Ink_{obs} = InA - E_a/RT \tag{10}$$

$$In\left(\frac{k_{obs}}{T}\right) = -\frac{\Delta H^{\ddagger}}{RT} + In\left(\frac{k_B}{h}\right) + \frac{\Delta S^{\ddagger}}{R} \tag{11}$$

Equation (9) describes the Arrhenius equation [71] which was linearized to the form shown in **Equation (10)** while **Equation (11)** describes the Eyring equation [74]. A is the Arrhenius constant or frequency factor (min^{-1}), E_a is the activation energy (J/mol), R is the universal gas constant (8.314 J/mol.K), T is the absolute temperature (K), $\Delta H^{\ddagger}$ is the enthalpy of activation (J/mol), k_B is the Boltzmann's constant (1.380649 x 10^{-23} J/K), h is the Planck's constant (6.62607015 x 10^{-34} J. s), and $\Delta S^{\ddagger}$ is the entropy of activation (J/mol·K). The superscripted notation (‡) refers to the value of interest in the activation complex or transition state [75].

The Gibb's free energy of activation ($\Delta G^{\ddagger}$) was determined for all temperatures by the thermodynamics fundamental equation [76]:

$$\Delta G^{\ddagger} = \Delta H^{\ddagger} - T\Delta S^{\ddagger} \tag{12}$$

A series of reactions were conducted using DMAP/DPTU binary catalyst and 100 % CO_2 while varying the reaction temperature within 40 – 80 °C (other conditions: 0.5 mol/L DMAP, 0.066 mol/L DPTU, and 8.11 mol/L ECH). To evaluate the influence of DPTU on the kinetics and thermodynamic activation parameters another series of reactions were conducted using DMAP only and 100 % CO_2, while varying the reaction temperature within 40 – 80 °C (other conditions: 0.5 mol/L DMAP and 8.11 mol/L ECH). Fig. 8 shows linear kinetic graphs (R^2 ≥ 0.993) from fitting experimental data to the pseudo first-order kinetic model for temperatures 40 – 80 °C, illustrating temperature dependency of reaction rate. The values of k_{obs} were 0.0025 min^{-1}, 0.0041 min^{-1}, 0.0067 min^{-1}, 0.0091 min^{-1}, and 0.0129 min^{-1} at 40 °C, 50 °C, 60 °C, 70 °C, and 80 °C, respectively for DMAP/DPTU and 100 % CO_2. On the other hand, the values of k_{obs} were 0.0016 min^{-1}, 0.0025 min^{-1}, 0.0044 min^{-1}, 0.0077 min^{-1}, and 0.0105 min^{-1} at 40 °C, 50 °C, 60 °C, 70 °C, and 80 °C, respectively for DMAP only and 100 % CO_2. These results imply that, as temperature increased from 40 °C to 80 °C, the reaction rate increased by a factor of 5 in the presence of DMAP/DPTU binary catalyst and 100 % CO_2, whereas the reaction rate increased by a factor of 7 in the presence of DMAP only and 100 % CO_2. These trends demonstrate a positive correlation between reaction rate and temperature within 40 – 80 °C.

The activation energy (E_a) for CO_2 cycloaddition to ECH in the presence of either DMAP/DPTU or DMAP only was determined from the linear Arrhenius plots (ln k_{obs} versus 1/T) of Fig. 9, over the temperature range of 40 – 80 °C. E_a was found to be 37.61 kJ/mol in the presence of DMAP/DPTU and 100 % CO_2, while its value E_a was 44.98 kJ/mol in the presence of DMAP only and 100 % CO_2 (Table 2). The value of E_a decreased by 7.37 kJ/mol as a result of the synergistic catalytic action of DMAP and DPTU. This shows that the presence of DPTU reduced the energy barrier for the reaction, thereby accelerating the reaction rate between ECH and CO_2 as observed from the k_{obs} values for the reactions catalyzed by DMAP/DPTU binary catalyst compared to those catalyzed by DMAP only.

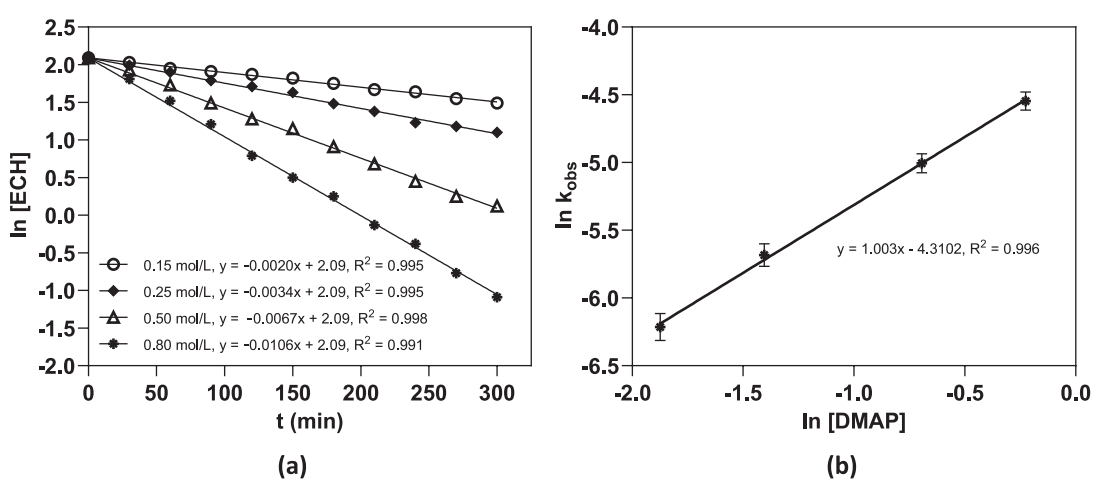

Fig. 6. Determination of reaction order in DMAP concentration: (a) plot showing linear fit of experimental data for [DMAP] = 0.15 – 0.80 mol/L into pseudo first-order kinetics, (b) Plot of In k_{obs} versus In [DMAP] to determine reaction order in [DMAP]. Error bar represents the standard deviation.

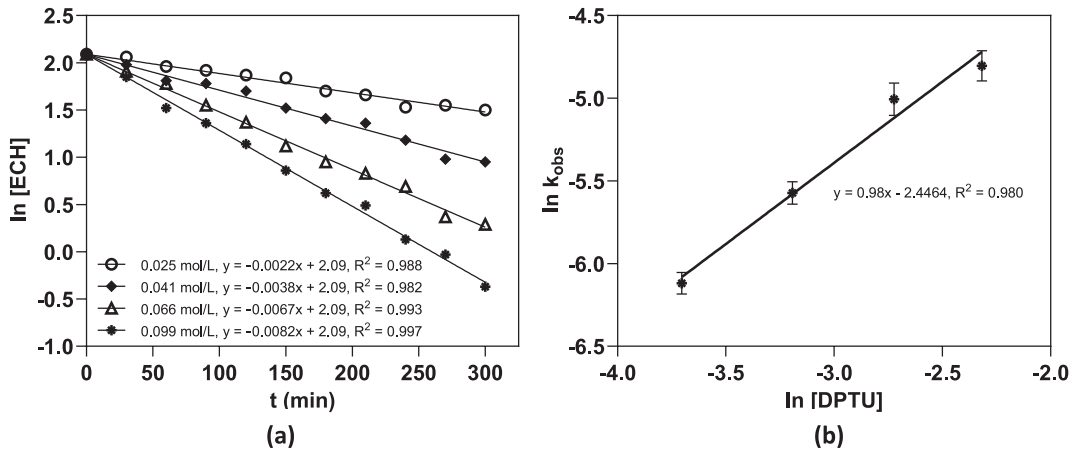

Fig. 7. Determination of reaction order in DPTU concentration: (a) plot showing linear fit of experimental data for [DPTU] = 0.025 – 0.099 mol/L into pseudo first-order kinetics, (b) plot of In k_{obs} versus In [DPTU] to determine reaction order in [DPTU]. Error bar represents the standard deviation.

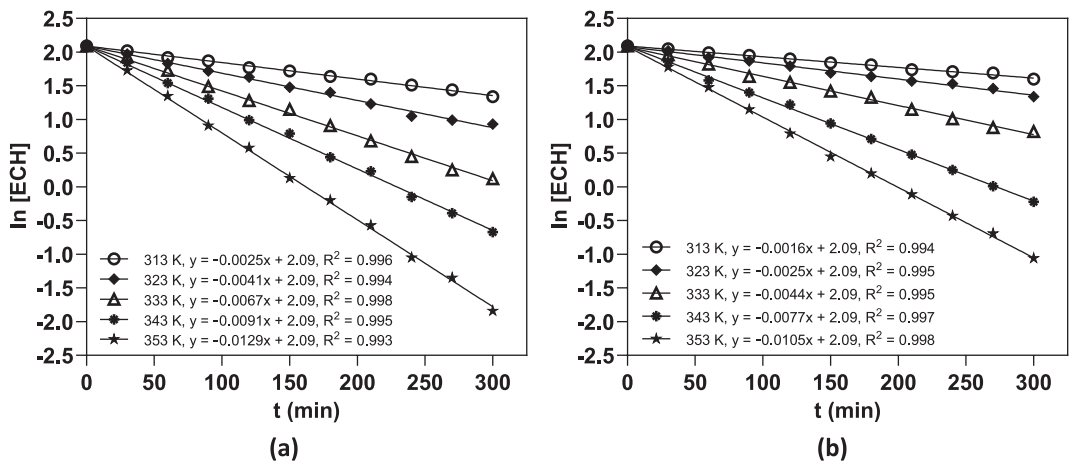

Fig. 8. Plots of In [ECH] versus t for T = 40 – 80 °C showing linear fit to pseudo first-order kinetics: (a) DMAP/DPTU binary catalyst and 100 % CO_2, (b) DMAP only and 100 % CO_2.

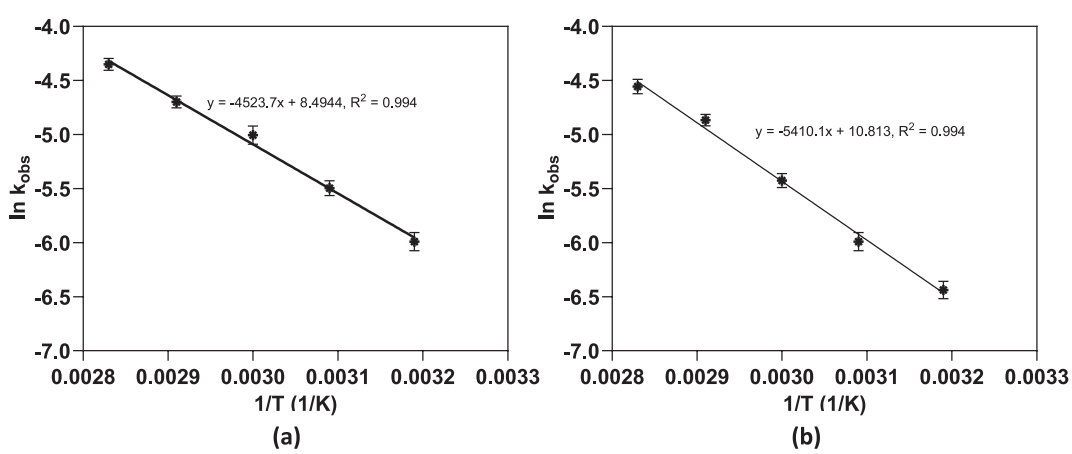

Fig. 9. Arrhenius plots for CO_2 cycloaddition to ECH: (a) DMAP/DPTU and 100% CO_2, (b) DMAP only and 100% CO_2.

Furthermore, the enthalpy of activation ($\Delta H^{\ddagger}$) and entropy of activation ($\Delta S^{\ddagger}$) in the presence of either DMAP/DPTU or DMAP only were determined from the linear Eyring plots (In (k_{obs}/T) versus 1/T) of Fig. 10 [77]. The Gibb's free energy of activation ($\Delta G^{\ddagger}$) was also determined.

Table 2 summarizes the values of $\Delta H^{\ddagger}$, $\Delta S^{\ddagger}$, and $\Delta G^{\ddagger}$ obtained and illustrates the influence of DPTU on these thermodynamic activation parameters.

In the presence of DMAP/DPTU binary catalyst and 100 % CO_2, the values of $\Delta H^{\ddagger}$ and $\Delta S^{\ddagger}$ were 34.85 kJ/mol and −0.22 kJ/mol.K, respectively while $\Delta G^{\ddagger}$ was in the range of 102.95 kJ/mol to 111.65 kJ/mol between 40 – 80 °C. However, in the presence of DMAP only and

Table 2
Influence of DPTU on Kinetics and Thermodynamic Activation Parameters for DMAP-based Catalysts[a], [b].

Parameter	DMAP/DPTU and 100 % CO_2	DMAP only and 100 % CO_2
E_a (kJ/mol)	37.61 ± 0.566	44.98 ± 1.697
$\Delta H^{\ddagger}$ (kJ/mol)	34.85 ± 1.131	42.22 ± 2.014
$\Delta S^{\ddagger}$ (kJ/mol. K)	−0.22 ± 0.010	−0.20 ± 0.011
$\Delta G^{\ddagger}$ (kJ/mol) at T =		
40 °C	102.95	104.28
50 °C	105.12	106.26
60 °C	107.30	108.25
70 °C	109.47	110.23
80 °C	111.65	112.21

[a] – Other reaction conditions: $[ECH]_o$ = 8.11 mol/L, [DMAP] = 0.5 mol/L, [DPTU] = 0.066 mol/L, t = 5 hr;
[b] – values are the mean of triplicate ± 1 standard deviation

100 % CO_2, the values of $\Delta H^{\ddagger}$ and $\Delta S^{\ddagger}$ were 42.22 kJ/mol and −0.20 kJ/mol. K, respectively while the value of the $\Delta G^{\ddagger}$ was in the range of 104.28 kJ/mol to 112.21 kJ/mol between 40 – 80 °C. The positive values of $\Delta H^{\ddagger}$ and $\Delta G^{\ddagger}$ reveal the non-spontaneous, endergonic, and chemically controlled nature of the cycloaddition reaction. Moreover, the negative values of $\Delta S^{\ddagger}$ indicate an ordered activated complex at the transition state.

The performance of the DMAP/DPTU binary catalyst in mediating CO_2 cycloaddition to ECH was compared to previously reported catalysts based on k_{obs} and E_a values in Table 3. For the identical reaction of CO_2 and ECH, catalysts derived from metal-organic complexes and halide salts were found to have first-order observed rate constants ranging from 0.0042 to 0.0070 min^{-1} at elevated reaction pressures of 9.9—29.6 atm and temperatures of 50—110 °C.

The DMAP/DPTU binary catalyst, on the other hand, achieved a comparable reaction rate (k_{obs} = 0.0067 min^{-1}) at atmospheric pressure (1 atm) and 60 °C. When a metal–organic complex [70] was used at 1

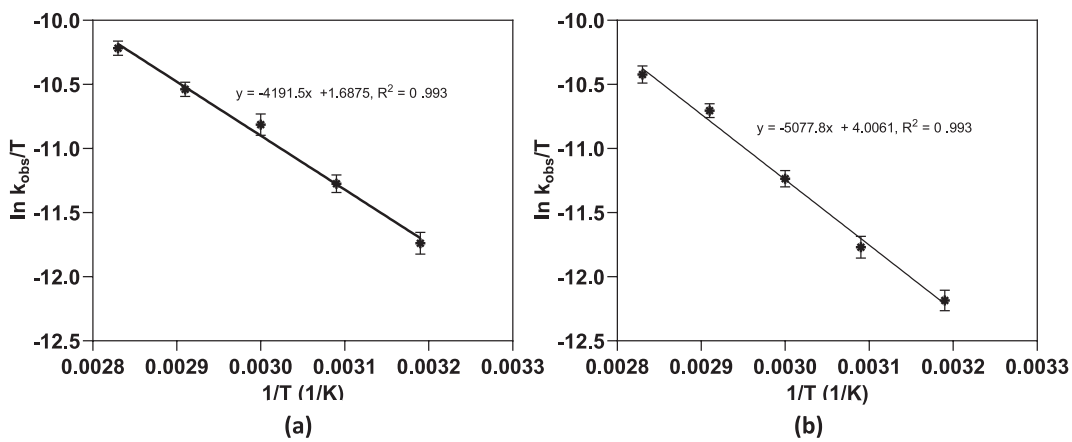

Fig. 10. Eyring plots for CO_2 cycloaddition to ECH: (a) DMAP/DPTU and 100% CO_2, (b) DMAP only and 100% CO_2.

Table 3
Comparison of the Rate Constant and Activation Energy for DMAP/DPTU Catalyzed Cycloaddition of CO_2 to ECH with other Catalytic Systems.

Entry	Catalyst	P (atm)	k_{obs} /T	E_a (kJ/mol)	T Range (°C)	Ref
1[a]	Nanocrystalline Li promoted magnesia	29.6	0.0067 min^{-1}/ 110 °C	63.35	110—140	[78]
2[a]	Bisimidazole-functionalized porphyrin Co(III) chloride	19.7	0.0042 min^{-1}/ 90 °C	46.10	90 – 120	[69]
3[a]	Hydroxy ionic liquid functionalized Zn porphyrin catalyst	9.9	0.0068 min^{-1}/ 80 °C	59.54	80—120	[72]
4[a]	Aluminum fumarate metal–organic framework /TBABr	9.9	0.0059 min^{-1}/ 50 °C	39.00	40—60	[79]
5[a]	Co(III) salen based complex/PPNY [c]	19.7	0.00087 min^{-1}/ 10 °C	98.50	10—25	[80]
6[a]	1, 3-bis(3-methylimidazolium-1-yl) hexane dibromide/ZnBr2	29.6	0.0070 min^{-1}/ 50 °C	32.00	50—90	[81]
7[a]	Cyclic polypyrazoles	9.9	0.0064 min^{-1}/ 60 °C	84.69	40—60	[82]
8[a]	Amino-functional ionic liquid	9.9	0.0152 min^{-1}/ 100 °C	45.90	100—130	[83]
9[a]	Polyhedral oligomeric silsesquioxane polyionic liquid	1	0.0430 min^{-1}/ 65 °C	41.25	65—90	[84]
10[a]	Amine-functionalized bimetallic Co/Zn-zeolitic imidazolate framework with 3-amino-1,2,4 triazole	1	0.0029 min^{-1}/ 80 °C	39.50	50—100	[70]
11[a]	DMAP/DPTU	1	0.0067 min^{-1}/ 60 °C	37.61	40—80	*This Work*
12[b]	DMAP/DPTU	1	0.0056 min^{-1}/ 60 °C	–	–	*This Work*

[a] – 100 % CO_2, reaction order = 1;
[b] – 15 % CO_2, reaction order = 1;
[c] – [PPN = bis(triphenylphosphine)iminium], [Y = 2,4-dinitrophenoxide].

atm and 80 °C, the reaction rate was reduced (k_{obs} = 0.0029 min^{-1}) compared to the DMAP/DPTU binary catalyst. Moreover, the DMAP/DPTU catalyzed reaction between ECH and CO_2 required a lower activation energy (37.61 kJ/mol) than many of the previously reported metal–organic complexes and halide salts-based catalysts. Thus, the current metal and halide-free catalytic strategy comprising a nucleophilic base (DMAP) and an N–H type HBD (DPTU) effectively promoted a reaction that requires less energy, resulting in faster kinetics that allowed high yields of CMEC under low CO_2 partial pressure of 0.15 atm.

3.4.5. Mechanistic Considerations

The role played by each catalytic component was examined to understand the mechanism of DMAP/DPTU-mediated reaction between CO_2 and ECH. The role of DPTU was hypothesized to be related to its capability to form hydrogen bonds with other molecules due to the presence of the amino (N–H) group in its structure. Therefore, ^{1}H NMR technique was used to probe the existence of such hydrogen bonding interactions between the DPTU molecule and the other components of the reaction system by monitoring the variation of the chemical shift of the protons [28,85]. As shown in Fig. 11, when a room-temperature mixture of DPTU and ECH in $CDCl_3$ was analyzed, the ^{1}H NMR spectra of the mixture revealed a downfield shift of the N–H proton signal of DPTU from δ of 7.80 ppm to 8.10 ppm (Fig. 11 **a and c**). In addition, the aromatic proton signals of DPTU (labelled as **2** at δ of 7.28 – 7.46 ppm in Fig. 11**a**) also shifted upfield by approximately 0.05 ppm as a result of the deformation of electron density around the aromatic rings of DPTU. These variations in proton chemical shifts may presumably be caused by hydrogen bonding interaction between the N–H proton of DPTU and oxygen atom of ECH. This supports the hypothesis that the co-catalytic role of DPTU derives from its capability to activate the ECH molecule through the coordination of N–H proton with the electron-rich oxygen atom of ECH via hydrogen bonding to facilitate a more effective ECH ring opening.

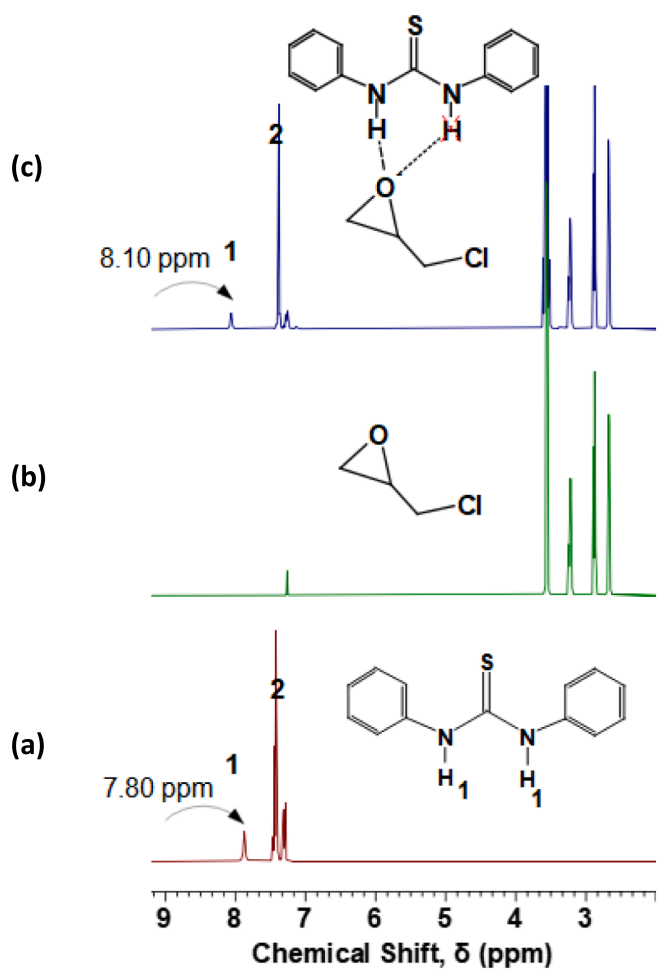

Fig. 11. ^{1}H NMR spectra in $CDCl_3$ at 298 K: (a) DPTU [10 wt% in $CDCl_3$], (b) epichlorohydrin [10 wt% in $CDCl_3$], (c) epichlorohydrin/DPTU [1:1 wt ratio, 10 wt% in $CDCl_3$].

Furthermore, bases have been effective catalysts in reactions involving CO_2 and, interestingly, they have been thought to play varied roles in these reactions. Bases were reported for the trapping and subsequent transfer of CO_2 through the formation of a base-CO_2 adduct (carbamic complex) [86]. Nucleophilic catalysis by the base-CO_2 adducts in CO_2 reactions has also been reported [33,87]. Also, there have been examples of the bases themselves acting as nucleophiles in CO_2 reactions [88,89]. It was therefore envisioned that the catalytic role of DMAP in the cycloaddition of CO_2 to ECH could be based on one or combination of the following mechanisms: (1) DMAP activates CO_2 by attacking its electrophilic carbon to form an activated complex (carbamic complex) which acts as either a 'CO_2 carrier' or a nucleophile in the reaction (Fig. 12**a**) and (2) DMAP could act as a nucleophile in its bare form to attack ECH (Fig. 12**b**).

^{13}C NMR spectroscopy was applied to investigate the formation of the activated complexes of Fig. 12 in the reaction systems. First, a two-stage sequential process was implemented such that; (1) in the first stage, CO_2 could be pre-captured to form a carbamic complex, and (2) in the second stage, the pre-captured CO_2 could react with ECH to form CMEC. Consequently, CO_2 was bubbled through a mixture of DMAP/PEG_{200} at room temperature for 2 h and upon shutting off CO_2 gas, ECH was added to the pre-captured CO_2 and the mixture was stirred at 120 °C for 24 h. The formation of a carbamic complex during the first stage could be monitored through the appearance of the carbamic carbon (N-**C**OO$^-$) signal at chemical shift around 158.5——160.7 ppm [90], while the formation of CMEC could be monitored through the carbonyl carbon (**C** = O) signal at chemical shift of approximately 154.07 ppm. No extra carbon signal belonging to a carbamic carbon was observed on the ^{13}C NMR spectra of the mixture from stage 1 (***See Supplementary Material Figure S4***)**.** Also, no signal belonging to the carbonyl carbon of CMEC was observed on the ^{13}C NMR spectra of the mixture obtained from stage 2 (***See Supplementary Material Figure S4***). **Also,** TGA data showed that between 30 – 110 °C, there was no significant difference in weight loss between the mixture before and after the first stage (***See Supplementary Material Figure S5***), indicating that there was no appreciable capture of CO_2 by DMAP/PEG_{200}, hence the absence of the carbamic carbon signal on ^{13}C NMR spectra. These results strongly negate the formation of a carbamic complex in the catalytic cycle and mechanism 1 could be disregarded. Furthermore, ^{1}H NMR analysis of an ECH/DMAP mixture revealed the splitting of the signal of the methyl chloride (CH_2Cl) protons of ECH from a doublet at δ of 3.55 – 3.57 ppm (ECH only) to a multiplet at δ of 3.51 – 3.59 ppm (ECH/DMAP) (***See Supplementary Material Figure S6***). This observation indicates an interaction between ECH and DMAP and such interaction is expected to arise from the nucleophilic attack of DMAP on ECH forming the open ring complex of Fig. 12**b**.

Important observations derived from the kinetics investigations include (1) DMAP and DPTU each exerted a direct catalytic influence on the reaction as k_{obs} was directly proportional to the concentration of each component, (2) the reaction order with respect to DMAP and DPTU (order = 1) suggested the participation of one molecule of each per molecule of ECH in the catalytic cycle, (3) experimental evidence suggested the existence of interaction between the N–H proton of DPTU with ECH molecule through hydrogen bond coordination, and (4) experimental evidence showed the existence of interaction between DMAP and ECH molecules which is suspected to arise from the nucleophilic attack of DMAP on the electrophilic carbon atom of ECH. Based on these observations and previous studies, the reaction mechanism of Fig. 13 was proposed involving a synergistic catalytic action between

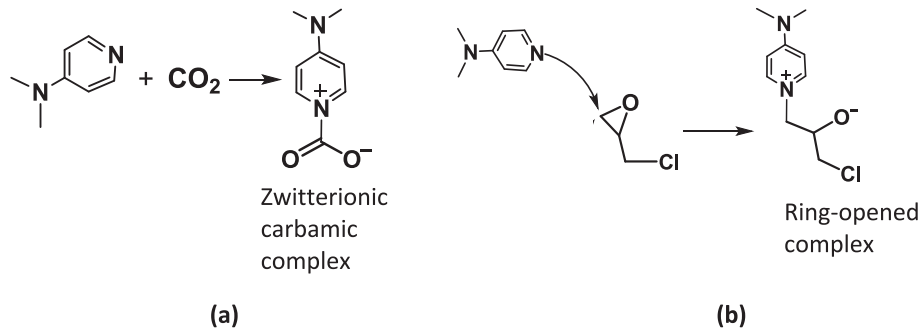

Fig. 12. Possible activated complexes from the interaction of DMAP with CO_2 or ECH.

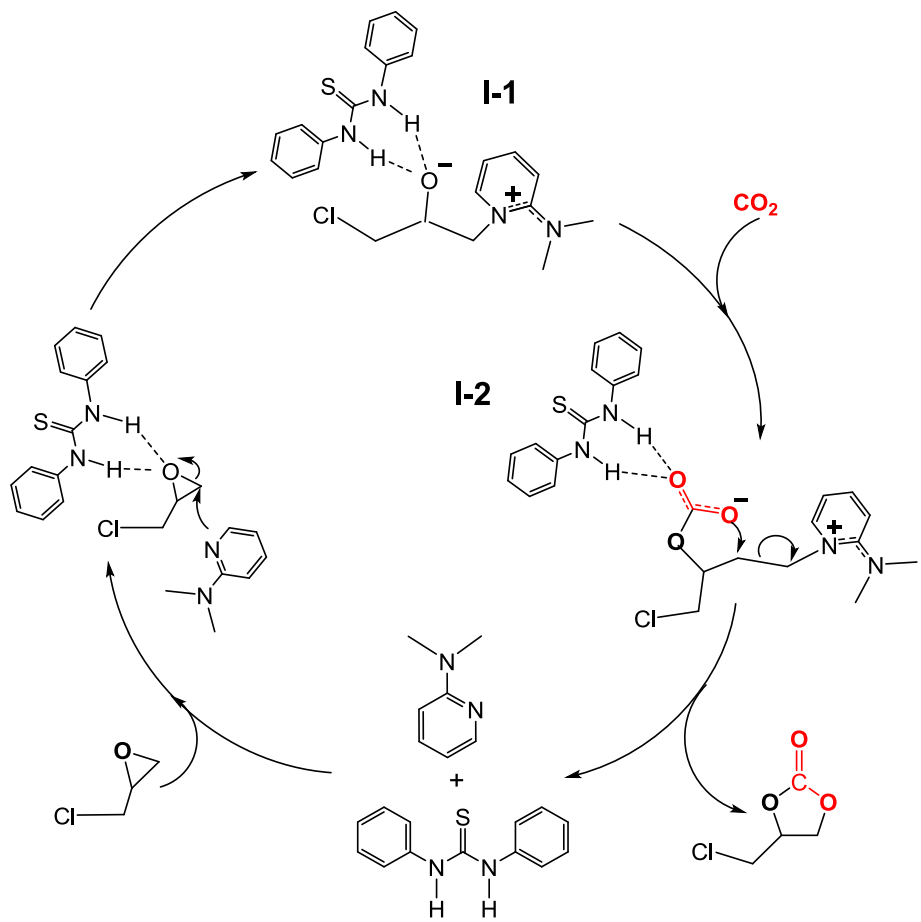

Fig. 13. Proposed reaction mechanism for CO_2 cycloaddition to ECH catalyzed by DMAP/DPTU binary catalyst.

DMAP and DPTU. DPTU activates the ECH molecule via hydrogen bond coordination. The nucleophilic DMAP then attacks the activated ECH molecule, opening its ring and forming an oxy-anion complex (**I-I**). Previous studies identified the ring opening step as the rate-determining step [91–93]. Indeed, the reaction seldom occurred in the absence of DMAP due to the lack of a nucleophilic specie to open the ECH ring. Combining DPTU with DMAP reduced the activation energy by 7.37 kJ/mol suggesting that the activation of ECH molecule by DPTU promoted a less energy-demanding and more facile opening of ECH ring leading to faster kinetics. The oxy-anion complex attacks CO_2 on its electrophilic carbon atom and the whole CO_2 molecule is incorporated to form a carbonate complex (**I-2**) which undergoes a re-arrangement to form CMEC and regenerate the catalysts to complete the catalytic cycle.

4. Conclusion

Synthesis of CMEC via the reaction of ECH and CO_2 was achieved by a metal-free and halide-free catalytic methodology involving a combination of cheap and readily DMAP and N–H containing HBDs, namely urea, thiourea, DPU, and DPTU. At a low concentration of 0.025 w/w relative to ECH, these N–H type HBDs enhanced the yield of CMEC, indicating a positive synergy with DMAP. The DMAP/DPTU binary catalyst showed superior catalytic activity among the catalytic combinations studied. The DMAP/DPTU binary catalyst remained sufficiently active under a 15 % CO_2/85 % N_2 (v/v) simulated flue gas atmosphere to produce CMEC at low temperatures of 30 – 60 °C, and interestingly, achieved a high CMEC yield and selectivity of 93 % and 98 %, respectively at 40 °C after 24 h. The DMAP/DPTU binary catalyst was stable in the presence of 5 % O_2 (v/v) in the simulated flue gas showing no decline

in activity. However, a high concentration of H_2O in the reactor had a negative effect on CMEC yield and selectivity. Regarding other flue gas constituents, further work is required to assess the impact SO_2 and NO_x, but ideally these need to be reduced to ppm levels to ensure the reaction is not adversely affected. The reaction of ECH and CO_2 was pseudo first-order in ECH concentration. The catalytic cycle involved one molecule each of the HBD (DPTU) and base (DMAP). The catalyst composition, CO_2 partial pressure, and temperature were significant factors that controlled the reaction rate. The presence of DPTU accelerated the reaction rate by a factor of 1.52 while a decrease in CO_2 partial pressure from 1 to 0.15 atm decreased the reaction rate by a factor of 0.84. DPTU decreased E_a by 7.37 kJ/mol according to the Arrhenius model. The values of $\Delta H^{\ddagger}$ and $\Delta G^{\ddagger}$ were positive, suggesting that the reaction was endergonic and kinetically controlled. A synergistic reaction mechanism was proposed in which DPTU activates the ECH by hydrogen bond coordination, while DMAP opens the ring of the activated ECH by nucleophilic attack, allowing the CO_2 molecule to be incorporated into the open-ring intermediate to form CMEC.

CRediT authorship contribution statement

Udeme O. Eton: Writing – review & editing, Writing – original draft, Methodology, Investigation, Formal analysis, Data curation, Conceptualization. **Will Meredith:** Writing – review & editing, Supervision. **Colin E. Snape:** Writing – review & editing, Supervision.

Declaration of competing interest

The authors declare that they have no known competing financial interests or personal relationships that could have appeared to influence the work reported in this paper.

Acknowledgements

The authors wish to acknowledge Nigeria's Government for sponsoring Udeme's PhD research through a grant from Tetiary Education Trust Fund (TETFund) (Grant Number: TETF/ES/UNIV/AKWA IBOM/ASTD/2018).

Appendix A. Supplementary data

Supplementary data to this article can be found online at https://doi.org/10.1016/j.fuel.2024.133657.

Data availability

Data will be made available on request.

References

[1] Aresta M, Dibenedetto A. Utilisation of CO2 as a chemical feedstock: Opportunities and challenges. *Dalton Trans* Published online June 26 2007:2975–92. https://doi.org/10.1039/b700658f.
[2] Challa P, Paleti G, Madduluri VR, et al. Trends in emission and utilization of CO2: sustainable feedstock in the synthesis of value-added fine chemicals. Catal Surv Asia 2022;26:80–91. https://doi.org/10.1007/s10563-021-09352-6.
[3] Chauvy R, Meunier N, Thomas D, De Weireld G. Selecting emerging CO2 utilization products for short- to mid-term deployment. Appl Energy 2019;236:662–80. https://doi.org/10.1016/j.apenergy.2018.11.096.
[4] Otto A, Grube T, Schiebahn S, Stolten D. Closing the loop: Captured CO2 as a feedstock in the chemical industry. Energy Environ Sci 2015;8(11):3283–97. https://doi.org/10.1039/c5ee02591e.
[5] Zhang Z, Pan SY, Li H, et al. Recent advances in carbon dioxide utilization. Renew Sustain Energy Rev 2020;125:109799. https://doi.org/10.1016/j.rser.2020.109799.
[6] Hasan MMF, Rossi LM, Debecker DP, et al. Can CO2 and renewable carbon be primary resources for sustainable fuels and chemicals? ACS Sustain Chem Eng 2021;9:12427–30. https://doi.org/10.1021/acssuschemeng.1c06008.
[7] Godin J, Liu W, Ren S, Xu CC. Advances in recovery and utilization of carbon dioxide: A brief review. J Environ Chem Eng 2021;9:105644. https://doi.org/10.1016/j.jece.2021.105644.
[8] IEA. *Putting CO2 to Use. Creating Value from Emissions*.; 2019. Accessed November 25, 2023. https://www.iea.org/reports/putting-co2-to-use.
[9] Bhattacharyya D, Miller DC. Post-combustion CO2 capture technologies — a review of processes for solvent-based and sorbent-based CO2 capture. Curr Opin Chem Eng 2017;17:78–92. https://doi.org/10.1016/j.coche.2017.06.005.
[10] Liang Z, Fu K, Idem R, Tontiwachwuthikul P. Review on current advances, future challenges and consideration issues for post-combustion CO2 capture using amine-based absorbents. Chin J Chem Eng 2016;24:278–88. https://doi.org/10.1016/j.cjche.2015.06.013.
[11] Álvarez A, Borges M, Corral-Pérez JJ, et al. CO2 activation over catalytic surfaces. ChemPhysChem 2017;18(22):3135–41. https://doi.org/10.1002/cphc.201700782.
[12] Baki ZA, Dib H, Sahin T. Overview: polycarbonates via ring-opening polymerization, differences between six- and five-membered cyclic carbonates: inspiration for green alternatives. Polymers (Basel) 2022;14:2031. https://doi.org/10.3390/polym14102031.
[13] Pescarmona PP. Cyclic carbonates synthesised from CO2: Applications, challenges and recent research trends. Curr Opin Green Sustain Chem 2021;29:100457. https://doi.org/10.1016/j.cogsc.2021.100457.
[14] Schäffner B, Schäffner F, Verevkin SP, Börner A. Organic carbonates as solvents in synthesis and catalysis. Chem Rev 2010;110(8):4554–81. https://doi.org/10.1021/cr900393d.
[15] Fukuoka S, Tojo M, Hachiya H, Aminaka M, Hasegawa K. Green and sustainable chemistry in practice: development and industrialization of a novel process for polycarbonate production from CO2 without using phosgene. Polym J 2007;37(2):91–114. https://doi.org/10.1295/polymj.PJ2006140.
[16] He X, Chen D, Liang Z, Yang F. Insight and comparison of energy-efficient membrane processes for CO2 capture from flue gases in power plant and energy-intensive industry. Carbon Capture Sci Technol 2022;2:100020. https://doi.org/10.1016/j.ccst.2021.100020.
[17] Pohlmann J, Bram M, Wilkner K, Brinkmann T. Pilot scale separation of CO2 from power plant flue gases by membrane technology. Int J Greenhouse Gas Control 2016;53:56–64. https://doi.org/10.1016/j.ijggc.2016.07.033.
[18] Castro-Osma JA, Lara-Sánchez A, North M, Otero A, Villuendas P. Synthesis of cyclic carbonates using monometallic, and helical bimetallic, aluminium complexes. Catal Sci Technol 2012;2(5):1021–6. https://doi.org/10.1039/c2cy00517d.
[19] Chen Y, Luo R, Xu Q, Zhang W, Zhou X, Ji H. State-of-the-art aluminum porphyrin-based heterogeneous catalysts for the chemical fixation of CO2 into cyclic carbonates at ambient conditions. ChemCatChem 2017;9(5):767–73. https://doi.org/10.1002/cctc.201601578.
[20] Clegg W, Harrington RW, North M, Pasquale R. Cyclic carbonate synthesis catalysed by bimetallic aluminium-salen complexes. Chem A Eur J 2010;16:6828–43. https://doi.org/10.1002/chem.201000030.
[21] Liang J, Xie YQ, Wu Q, et al. Zinc porphyrin/imidazolium integrated multivariate zirconium metal−organic frameworks for transformation of CO2 into cyclic carbonates. Inorg Chem 2018;57:2584–93. https://doi.org/10.1021/acs.inorgchem.7b02983.
[22] Meléndez J, North M, Pasquale R. Synthesis of cyclic carbonates from atmospheric pressure carbon dioxide using exceptionally active aluminium(salen) complexes as catalysts. Eur J Inorg Chem 2007;2007(21):3323–6. https://doi.org/10.1002/ejic.200700521.
[23] North M. Synthesis of cyclic carbonates from epoxides and carbon dioxide using bimetallic aluminium(salen) complexes. *ARKIVOC* 2012;2012:610–28. https://doi.org/10.3998/ark.5550190.0013.115.
[24] Peng J, Geng Y, Yang HJ, et al. Efficient solvent-free fixation of CO2 into cyclic carbonates catalyzed by Bi(III) porphyrin/TBAI at atmospheric pressure. Mol Catal 2017;432:37–46. https://doi.org/10.1016/j.mcat.2017.01.019.
[25] Meléndez J, North M, Villuendas P. One-component catalysts for cyclic carbonate synthesis. Chem Commun 2009;18:2577–9. https://doi.org/10.1039/b900180h.
[26] Meléndez J, North M, Villuendas P, Young C. One-component bimetallic aluminium(salen)-based catalysts for cyclic carbonate synthesis and their immobilization. Dalton Trans 2011;40(15):3885–902. https://doi.org/10.1039/c0dt01196g.
[27] Parmar B, Patel P, Pillai RS, Kureshy RI, Khan NUH, Suresh E. Efficient catalytic conversion of terminal/internal epoxides to cyclic carbonates by porous Co(ii) MOF under ambient conditions: Structure-property correlation and computational studies. J Mater Chem A Mater 2019;7(6):2884–94. https://doi.org/10.1039/c8ta10631b.
[28] Arayachukiat S, Kongtes C, Barthel A, et al. Ascorbic acid as a bifunctional hydrogen bond donor for the synthesis of cyclic carbonates from CO2 under ambient conditions. ACS Sustain Chem Eng 2017;5(8):6392–7. https://doi.org/10.1021/acssuschemeng.7b01650.
[29] Gong Q, Luo H, Cao D, Zhang H, Wang W, Zhou X. Efficient cycloaddition reaction of carbon dioxide with epoxide by Rhodamine based catalyst under 1 atm pressure. Bull Korean Chem Soc 2012;33(6):1945–8. https://doi.org/10.5012/bkcs.2012.33.6.1945.
[30] Hardman-Baldwin AM, Mattson AE. Silanediol-catalyzed carbon dioxide fixation. ChemSusChem 2014;7(12):3275–8. https://doi.org/10.1002/cssc.201402783.
[31] Liu S, Suematsu N, Maruoka K, Shirakawa S. Design of bifunctional quaternary phosphonium salt catalysts for CO2 fixation reaction with epoxides under mild conditions. Green Chem 2016;18(17):4611–5. https://doi.org/10.1039/c6gc01630h.
[32] Wang X, Wang L, Zhao Y, Kodama K, Hirose T. Efficient and practical organocatalytic system for the synthesis of cyclic carbonates from carbon dioxide

and epoxides: 3-hydroxypyridine/tetra-n-butylammonium iodide. Tetrahedron 2017;73(8):1190–5. https://doi.org/10.1016/j.tet.2017.01.018.
[33] Wang L, Zhang G, Kodama K, Hirose T. An efficient metal- and solvent-free organocatalytic system for chemical fixation of CO2 into cyclic carbonates under mild conditions. Green Chem 2016;18(5):1229–33. https://doi.org/10.1039/c5gc02697k.
[34] Aoyagi N, Furusho Y, Endo T. Remarkably efficient catalysts of amidine hydroiodides for the synthesis of cyclic carbonates from carbon dioxide and epoxides under mild conditions. Chem Lett 2012;41(3):240–1. https://doi.org/10.1246/cl.2012.240.
[35] Fanjul-Mosteirín N, Jehanno C, Ruipérez F, Sardon H, Dove AP. Rational study of DBU salts for the CO2 insertion into epoxides for the synthesis of cyclic carbonates. ACS Sustain Chem Eng 2019;7:10633–40. https://doi.org/10.1021/acssuschemeng.9b01300.
[36] Kumatabara Y, Okada M, Shirakawa S. Triethylamine hydroiodide as a simple yet effective bifunctional catalyst for CO 2 fixation reactions with epoxides under mild conditions. ACS Sustain Chem Eng 2017;5:7295–301. https://doi.org/10.1021/acssuschemeng.7b01535.
[37] Zhao TX, Zhang YY, Liang J, Li P, Hu XB, Wu YT. Multisite activation of epoxides by recyclable CaI2/N-methyldiethanolamine catalyst for CO2 fixation: A facile access to cyclic carbonates under mild conditions. Mol Catal 2018;450:87–94. https://doi.org/10.1016/j.mcat.2018.03.010.
[38] Wang L, Kodama K, Hirose T. DBU/benzyl bromide: An efficient catalytic system for the chemical fixation of CO2 into cyclic carbonates under metal- and solvent-free conditions. Catal Sci Technol 2016;6(11):3872–7. https://doi.org/10.1039/c5cy01892g.
[39] Dai Z, Sun Q, Liu X, et al. Metalated porous porphyrin polymers as efficient heterogeneous catalysts for cycloaddition of epoxides with CO2 under ambient conditions. J Catal 2016;338:202–9. https://doi.org/10.1016/j.jcat.2016.03.005.
[40] Ding M, Jiang HL. Incorporation of Imidazolium-Based Poly(ionic liquid)s into a metal-organic framework for CO2 capture and conversion. ACS Catal 2018;8(4):3194–201. https://doi.org/10.1021/acscatal.7b03404.
[41] Hui W, He XM, Xu XY, et al. Highly efficient cycloaddition of diluted and waste CO2 into cyclic carbonates catalyzed by porous ionic copolymers. J CO2 Util 2020;36:169–76. https://doi.org/10.1016/j.jcou.2019.11.003.
[42] Metcalfe IS, North M, Pasquale R, Thursfield A. An integrated approach to energy and chemicals production. Energy Environ Sci 2010;3(2):212–5. https://doi.org/10.1039/b918417a.
[43] North M, Villuendas P, Young C. A gas-phase flow reactor for ethylene carbonate synthesis from waste carbon dioxide. Chem A Eur J 2009;15(43):11454–7. https://doi.org/10.1002/chem.200902436.
[44] Shen YM, Duan WL, Shi M. Chemical fixation of carbon dioxide co-catalyzed by a combination of Schiff bases or phenols and organic bases. European J Org Chem 2004;2004(14):3080–9. https://doi.org/10.1002/ejoc.200400083.
[45] Qi Y, Cheng W, Xu F, Chen S, Zhang S. Amino acids/superbases as eco-friendly catalyst system for the synthesis of cyclic carbonates under metal-free and halide-free conditions. Synth Commun 2018;48(8):876–86. https://doi.org/10.1080/00397911.2017.1339802.
[46] Liu Y, Li S, Chen Y, et al. Modified melamine-based porous organic polymers with imidazolium ionic liquids as efficient heterogeneous catalysts for CO2 cycloaddition. J Colloid Interface Sci 2023;652:737–48. https://doi.org/10.1016/j.jcis.2023.07.127.
[47] Jiang B, Liu J, Yang G, Zhang Z. Efficient conversion of CO2 into cyclic carbonates under atmospheric by halogen and metal-free poly(ionic liquid)s. Chin J Chem Eng 2023;55:202–11. https://doi.org/10.1016/j.cjche.2022.05.018.
[48] Ding J, Wang P, He Y, et al. Porous sulfonyl binuclear carbonate poly(ionic liquid)s for one-pot fixation of diluted CO2 into dimethyl carbonate. Appl Catal B 2023:324. https://doi.org/10.1016/j.apcatb.2022.122278.
[49] Qu Q, Cheng L, Wang P, et al. Guanidine-functionalized basic binuclear poly(ionic liquid)s for low partial pressure CO2 fixation into cyclic carbonate. Sep Purif Technol 2024;339. https://doi.org/10.1016/j.seppur.2024.126682.
[50] Zhou H, Wang GX, Zhang WZ, Lu XB. CO2 adducts of phosphorus ylides: highly active organocatalysts for carbon dioxide transformation. ACS Catal 2015;5:6773–9. https://doi.org/10.1021/acscatal.5b01409.
[51] Zhang J, Li X, Zhu Z, et al. Hydroxylamino-anchored poly(Ionic Liquid)s for CO2 fixation into cyclic carbonates at mild conditions. Adv Sustain Syst 2021;5(1). https://doi.org/10.1002/adsu.202000133.
[52] Castro-Osma JA, North M, Wu X. Synthesis of cyclic carbonates catalysed by chromium and aluminium salphen complexes. Chem A Eur J 2016;22:2100–7. https://doi.org/10.1002/chem.201504305.
[53] Zhang Z, Fan F, Xing H, Yang Q, Bao Z, Ren Q. Efficient synthesis of cyclic carbonates from atmospheric CO 2 using a positive charge delocalized ionic liquid catalyst. ACS Sustain Chem Eng 2017;5:2841–6. https://doi.org/10.1021/acssuschemeng.7b00513.
[54] Jiang X, Gou F, Qi C. C 2v -symmetric metalloporphyrin promoted cycloaddition of epoxides with CO 2 under atmospheric pressure. J CO2 Util 2019;29:134–9. https://doi.org/10.1016/j.jcou.2018.12.003.
[55] Chen XC, Zhao KC, Yao YQ, Lu Y, Liu Y. Synergetic activation of CO2by the DBU-organocatalyst and amine substrates towards stable carbamate salts for synthesis of oxazolidinones. Catal Sci Technol 2021;11(21):7072–82. https://doi.org/10.1039/d1cy01298c.
[56] Ji L, Luo Z, Zhang Y, et al. Imidazolium ionic liquids/organic bases: Efficient intermolecular synergistic catalysts for the cycloaddition of CO2 and epoxides under atmospheric pressure. Mol Catal 2018;446:124–30. https://doi.org/10.1016/j.mcat.2017.12.026.
[57] Robards K, Haddad PR, Jackson PE. Principles and practice of modern chromatographic methods. London: Elsevier Academic Press; 2004.
[58] Capoun T, Krykorkova J. Internal standards for quantitative analysis of chemical warfare agents by the GC/MS method: nerve agents. J Anal Methods Chem 2020. https://doi.org/10.1155/2020/8857210.
[59] ICH. *INTERNATIONAL CONFERENCE ON ICH HARMONISED TRIPARTITE GUIDELINE VALIDATION OF ANALYTICAL PROCEDURES: TEXT AND METHODOLOGY Q2(R1)*.; 2015. Accessed September 18, 2023. https://www.ich.org/fileadmin/PublicWebSite/ICHProducts/ Guidelines/Quality/Q2R1/Step4/Q2R1Guideline.pdf.
[60] Sakakura A, Kawajiri K, Ohkubo T, Kosugi Y, Ishihara K. Widely useful DMAP-catalyzed esterification under auxiliary base- and solvent-free conditions. J Am Chem Soc 2007;129(47):14775–9. https://doi.org/10.1021/ja075824w.
[61] Spivey AC, Arseniyadis S. Nucleophilic catalysis by 4-(dialkylamino)pyridines revisited - The search for optimal reactivity and selectivity. Angewandte Chemie - International Edition 2004;43:5436–41. https://doi.org/10.1002/anie.200460373.
[62] Wang X, Zhao Y, Kodama K, Hirose T. Poly(4-vinylphenol)/tetra-n-butylammonium iodide: Efficient organocatalytic system for synthesis of cyclic carbonates from CO2 and epoxides. J Appl Polym Sci 2017;45189:1–7. https://doi.org/10.1002/app.45189.
[63] Li J, Jia D, Guo Z, et al. Imidazolinium based porous hypercrosslinked ionic polymers for efficient CO2 capture and fixation with epoxides. Green Chem 2017;19:2675–86. https://doi.org/10.1039/c7gc00105c.
[64] Li Z, Jiang J, Ma Z, Fajardo OA, Deng J, Duan L. Influence of flue gas desulfurization (FGD) installations on emission characteristics of PM2.5 from coal-fired power plants equipped with selective catalytic reduction (SCR). Environ Pollut 2017;230:655–62. https://doi.org/10.1016/j.envpol.2017.06.103.
[65] Drage TC, Snape CE, Stevens LA, et al. Materials challenges for the development of solid sorbents for post-combustion carbon capture. J Mater Chem 2012;22(7):2815–23. https://doi.org/10.1039/c2jm12592g.
[66] Bains P, Psarras P, Wilcox J. CO2 capture from the industry sector. Prog Energy Combust Sci 2017;63:146–72. https://doi.org/10.1016/j.pecs.2017.07.001.
[67] Supasitmongkol S, Styring P. A single centre aluminium(iii) catalyst and TBAB as an ionic organo-catalyst for the homogeneous catalytic synthesis of styrene carbonate. Catal Sci Technol 2014;4:1622–30. https://doi.org/10.1039/c3cy01015e.
[68] Rehman A, Eze VC, Resul MFMG, Harvey A. Kinetics and mechanistic investigation of epoxide/CO2 cycloaddition by a synergistic catalytic effect of pyrrolidinopyridinium iodide and zinc halides. Journal of Energy Chemistry 2019;37:35–42. https://doi.org/10.1016/j.jechem.2018.11.017.
[69] Jiang X, Gou F, Chen F, Jing H. Cycloaddition of epoxides and CO2 catalyzed by bisimidazole-functionalized porphyrin cobalt(III) complexes. Green Chem 2016;18(12):3567–76. https://doi.org/10.1039/c6gc00370b.
[70] Nguyen QT, Do XH, Cho KY, Lee YR, Baek KY. Amine-functionalized bimetallic Co/Zn-zeolitic imidazolate frameworks as an efficient catalyst for the CO2 cycloaddition to epoxides under mild conditions. J CO2 Util 2022;61:102061. https://doi.org/10.1016/j.jcou.2022.102061.
[71] Liu M, Liu B, Zhong S, Shi L, Liang L, Sun J. Kinetics and mechanistic insight into efficient fixation of CO2 to epoxides over N-heterocyclic compound/ZnBr 2 catalysts. Ind Eng Chem Res 2015;54(2):633–40. https://doi.org/10.1021/ie5042879.
[72] Chen Y, Chen C, Li X, et al. Hydroxyl-ionic liquid functionalized metalloporphyrin as an efficient heterogeneous catalyst for cooperative cycloaddition of CO2 with epoxides. J CO2 Util 2022;62:102107. https://doi.org/10.1016/j.jcou.2022.102107.
[73] Rehman A, Saleem F, Javed F, Qutab HG, Eze VC, Harvey A. Kinetic study for styrene carbonate synthesis via CO2 cycloaddition to styrene oxide using silica-supported pyrrolidinopyridinium iodide catalyst. J CO2 Util 2021;43:101379. https://doi.org/10.1016/j.jcou.2020.101379.
[74] Mostafa B, Habibi-Khorassani SM, Shahraki M. An experimental investigation of substituent effects on the formation of 2,3-dihydroquinazolin-4(1H)-ones: a kinetic study. J Phys Org Chem 2017;30:e3616.
[75] Ong LK, Kurniawan A, Suwandi AC, Lin CX, Zhao XS, Ismadji S. Transesterification of leather tanning waste to biodiesel at supercritical condition: Kinetics and thermodynamics studies. J Supercrit Fluids 2013;75:11–20. https://doi.org/10.1016/j.supflu.2012.12.018.
[76] Sivakumar P, Parthiban KS, Sivakumar P, Vinoba M, Renganathan S. Optimization of extraction process and kinetics of Sterculia foetida seed oil and its process augmentation for biodiesel production. *Ind Eng Chem Res* 2012;51:8992–8. https://doi.org/10.1021/ie300882t.
[77] Tan CP, Che Man, Selamat J, Yusoff MSA. Application of Arrhenius kinetics to evaluate oxidative stability in vegetable oils by isothermal differential scanning calorimetry. JAOCS, J Am Oil Chem Soc 2001;78(11):1133–8. https://doi.org/10.1007/s11746-001-0401-1.
[78] Rasal KB, Yadav GD, Koskinen R, Keiski R. Solventless synthesis of cyclic carbonates by direct utilization of CO2 using nanocrystalline lithium promoted magnesia. Mol Catal 2018;451:200–8. https://doi.org/10.1016/j.mcat.2018.01.012.
[79] Kim HS, Yu K, Puthiaraj P, Ahn WS. CO2 cycloaddition to epichlorohydrin over an aluminum fumarate metal-organic framework synthesized by a sonochemical route. Microporous Mesoporous Mater 2020:306. https://doi.org/10.1016/j.micromeso.2020.110432.
[80] Wu GP, Wei SH, Ren WM, Lu XB, Xu TQ, Darensbourg DJ. Perfectly alternating copolymerization of CO 2 and epichlorohydrin using cobalt(III)-based catalyst

systems. J Am Chem Soc 2011;133(38):15191–9. https://doi.org/10.1021/ja206425j.
[81] Jaiswal P, Varma MN. Catalytic performance of dicationic ionic liquids and ZnBr 2 in the reaction of epichlorohydrin and carbon dioxide: kinetic study. Catal Letters 2017;147(8):2067–76. https://doi.org/10.1007/s10562-017-2062-0.
[82] Lu Z, He J, Guo B, et al. Efficient homogenous catalysis of CO2 to generate cyclic carbonates by heterogenous and recyclable polypyrazoles. Chin J Chem Eng 2022;43:110–5. https://doi.org/10.1016/j.cjche.2022.01.009.
[83] Yue S, Song Q, Zang S, Deng G, Li J. Amino-functional ionic liquids as efficient catalysts for the cycloaddition of carbon dioxide to yield cyclic carbonates: catalytic and kinetic investigation. Aust J Chem 2018;71(6):407–15. https://doi.org/10.1071/CH17656.
[84] Xiao L, Lai Y, Song Q, Cai J, Zhao R, Hou L. POSS-based polyionic liquids for efficient CO2 cycloaddition reactions under solvent- and cocatalyst-free conditions at ambient pressure. Dalton Trans 2023;52(27):9282–93. https://doi.org/10.1039/d3dt01244a.
[85] Wu K, Su T, Hao D, et al. Choline chloride-based deep eutectic solvents for efficient cycloaddition of CO2 with propylene oxide. Chem Commun 2018;54(69):9579–82. https://doi.org/10.1039/C8CC04412K.
[86] Pérez ER, Odnicki Da Silva M, Costa VC, Rodrigues-Filho UP, Franco DW. Efficient and clean synthesis of N-alkyl carbamates by transcarboxylation and O-alkylation coupled reactions using a DBU-CO2 zwitterionic carbamic complex in aprotic polar media. Tetrahedron Lett 2002;43:4091–3.
[87] Liu X, Zhang S, Song QW, Liu XF, Ma R, He LN. Cooperative calcium-based catalysis with 1,8-diazabicyclo[5.4.0]-undec-7-ene for the cycloaddition of epoxides with CO2 at atmospheric pressure. Green Chem 2016;18(9):2871–6. https://doi.org/10.1039/c5gc02761f.
[88] García-Argüelles S, Ferrer ML, Iglesias M, Del Monte F, Gutiérrez MC. Study of superbase-based deep eutectic solvents as the catalyst in the chemical fixation of CO2 into cyclic carbonates under mild conditions. Materials 2017;10(7):759. https://doi.org/10.3390/ma10070759.
[89] Jessop PG, Mercer SM, Heldebrant DJ. CO2-triggered switchable solvents, surfactants, and other materials. Energy Environ Sci 2012;5:7240–53. https://doi.org/10.1039/c2ee02912j.
[90] Yang ZZ, He LN, Zhao YN, Li B, Yu B. CO 2 capture and activation by superbase/polyethylene glycol and its subsequent conversion. Energy Environ Sci 2011;4(10):3971–5. https://doi.org/10.1039/c1ee02156g.
[91] Castro-Gómez F, Salassa G, Kleij AW, Bo C. A DFT study on the mechanism of the cycloaddition reaction of CO 2 to epoxides catalyzed by Zn(Salphen) complexes. Chem A Eur J 2013;19(20):6289–98. https://doi.org/10.1002/chem.201203985.
[92] Wang JQ, Dong K, Cheng WG, Sun J, Zhang SJ. Insights into quaternary ammonium salts-catalyzed fixation carbon dioxide with epoxides. Catal Sci Technol 2012;2(7):1480–4. https://doi.org/10.1039/c2cy20103h.
[93] Wang JQ, Sun J, Cheng WG, Dong K, Zhang XP, Zhang SJ. Experimental and theoretical studies on hydrogen bond-promoted fixation of carbon dioxide and epoxides in cyclic carbonates. PCCP 2012;14(31):11021–6. https://doi.org/10.1039/c2cp41698k.